

FIGURE 15 Change of fluorescence intensity of tag-probe pairs from 4°C to 100°C (low to high) and from 100°C to 4°C (high to low) in 50 mM HEPES buffer (pH 7.2, 100 mM NaCl): [tag-probe pair] = 0.5  $\mu$ M. (a) tag-probe 2 pair, (b) tag-probe 4 pair.

response, binding affinity, and chemical stability. As a spacer between the N<sup>ε</sup>-chloroacetyl group and the original probe sequence, a single Gly residue was superior to 0 or 2 Gly residues. Thus, the probe peptide 2, having the 1 Gly spacer, binds more rapidly to the tag peptide than the probe peptides 1 and 3, with 0 and 2 Gly spacers, respectively. Both the previous noncrosslink-type and the present crosslink-type ZIP tag-probe pairs might facilitate the real-time imaging of target proteins without removal of excess probe molecules. Thus, the crosslink-type ZIP tag-probe pairs should be highly useful and valuable for studies of imaging of proteins in living cells.

## EXPERIMENTAL PROCEDURES

### General

HPLC was carried out on a reversed phase column with a LaChrom Elite HTA system (Hitachi). Matrix-assisted laser desorption/ionization time-of-flight mass spectrometry

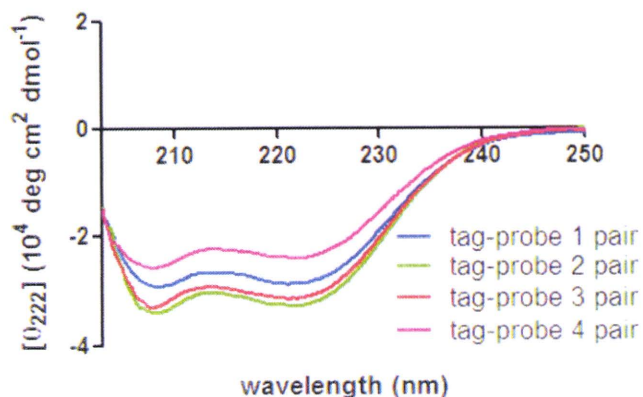


FIGURE 16 CD spectra of tag-probe pairs at 24°C in 50 mM Tris-HCl buffer (pH 7.2, 100 mM NaCl): [tag-probe pair] = 1  $\mu$ M. Tag-probe peptide 1 pair (blue), tag-probe peptide 2 pair (green), tag-probe peptide 3 pair (red) and tag-probe peptide 4 pair (magenta).

(MALDI-TOF-MS) was recorded on a Voyager DE-STR (Applied Biosciences) mass spectrometer. 3,5-dimethoxy-4-hydroxycinnamic acid was used as the matrix.

### Peptide Synthesis

Probe peptides 1-5 were synthesized by the Fmoc-based solid-phase method.<sup>26</sup> The tag peptide was prepared previously.<sup>20</sup> All peptides were purified by RP-HPLC and identified by MALDI-TOF-MS. Fmoc-protected amino acids and reagents for peptide synthesis were purchased from Novabiochem, Kokusan Chemical Co., Ltd. and Watanabe Chemical Industries, Ltd. Fmoc-Dap(NBD)-OH was synthesized as previously reported.<sup>30</sup> The probe peptides 1-5 were synthesized using NovaSyn TGR resin on a 0.1 mmol scale. All peptides were synthesized by stepwise elongation techniques of Fmoc-protected amino acids on the resin. The coupling reactions were performed using 5.0 equiv. of Fmoc-protected amino acid, 5.0 equiv. of diisopropylcarbodiimide (DIPCI) and 5.0 equiv. of 1-hydroxybenzotriazole monohydrate (HOBt·H<sub>2</sub>O) in DMF (5.0 mL). N-Terminal amino groups of the probe peptides 1-3 were chloroacetylated with chloroacetic acid, DIPCI and HOBt (5.0 equiv. each) in DMF (5.0 mL). N-Terminal amino groups of the probe peptides 4 and 5 were acetylated with acetic anhydride-DMF (1:4, v/v) (5.0 mL). In the synthesis of the probe peptide 5, Fmoc-Lys(Mtt)-OH (Mtt = 4-methyltrityl) was coupled as the C-terminal Fmoc-protected amino acid. After construction of the protected peptide 5 resin and N-terminal acetylation, the peptide 5 resin was treated by dichloromethane-triisopropylsilane-TFA (94:5:1, v/v) (2.0 mL) for 1 min, and this treatment was repeated 11 times,<sup>31</sup> followed by N<sup>ε</sup>-chloroacetylation with chloroacetic acid, DIPCI and HOBt (5.0 equiv. each) in DMF (5.0 mL). Cleavage and side chain deprotection of the probe peptides 1-5 was carried out with 10 mL of TFA in the presence of 0.25 mL of *m*-cresol, 0.75 mL of thioanisole, and 0.75 mL of 1,2-ethanedithiol as scavenger, by stirring for 1.5 h. After filtra-

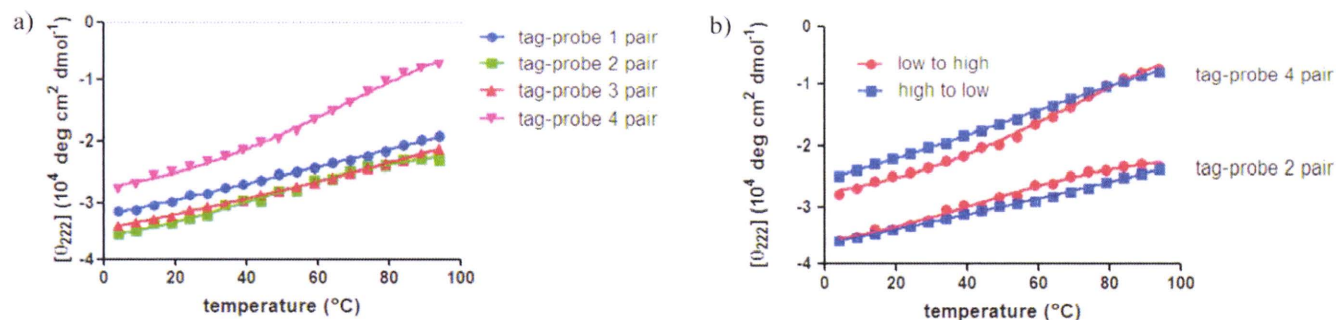


FIGURE 17 (a) Change of values of  $[\theta]$  at 222 nm of tag-probe pairs from 4°C to 94°C in 50 mM Tris-HCl buffer (pH 7.2, 100 mM NaCl):  $[\text{tag-probe pair}] = 1 \mu\text{M}$ . Tag-probe 1 pair (blue), tag-probe 2 pair (green), tag-probe 3 pair (red) and tag-probe 4 pair (magenta). (b) Change of values of  $[\theta]$  at 222 nm of tag-probe 2 and 4 pairs from 4°C to 94°C (low to high) (red) and from 94°C to 4°C (high to low) (blue) in 50 mM Tris-HCl buffer (pH 7.2, 100 mM NaCl).

tion, the reaction mixture was concentrated under reduced condition, and crude peptides were precipitated in cooled diethyl ether. All crude peptides were purified by RP-HPLC (column, YMC-Pack ODS-A,  $10\phi \times 250$  mm). The HPLC solvents employed were water containing 0.1% TFA (solvent A) and acetonitrile containing 0.1% TFA (solvent B). The probe peptides 1–5 was purified using a 23%–38% linear gradient of solvent B over 30 min. All purified peptides were identified by MALDI-TOF-MS. All peptides were obtained as TFA salts after lyophilization. Probe peptide 1, yield 21%,  $m/z$  2603.1, calcd 2603.5  $[\text{M} + \text{H}]^+$ . Probe peptide 2, yield 18%,  $m/z$  2661.1, calcd 2660.6  $[\text{M} + \text{H}]^+$ . Probe peptide 3, yield 23%,  $m/z$  2717.1, calcd 2717.6  $[\text{M} + \text{H}]^+$ . Probe peptide 4, yield 26%,  $m/z$  2627.0, calcd 2626.6  $[\text{M} + \text{H}]^+$ . Probe peptide 5, yield 7%,  $m/z$  2773.8, calcd 2773.7  $[\text{M} + \text{H}]^+$ .

### Crosslinking Reaction

The probe peptide (16 nmol) and tag peptide (16 nmol) were dissolved in 50 mM HEPES buffer, pH 7.2 containing 100 mM NaCl (16 mL), and incubated at room temperature in an  $\text{N}_2$  atmosphere. At intervals (0, 1, 5, 10, 15, 20, and 30 min), an aliquot (1.6 mL) was sampled and 10% aqueous AcOH (0.4 mL) was added to the aliquot. The reaction was traced by HPLC using a 20%–50% linear gradient of solvent B over 30 min. HPLC peaks of the starting compounds and the generated products were identified by MALDI-TOF-MS: tag-probe peptide 1,  $m/z$  7880.4, calcd 7877.2  $[\text{M} + \text{H}]^+$ . Tag-probe peptide 2,  $m/z$  7935.7, calcd 7934.2  $[\text{M} + \text{H}]^+$ . Tag-probe peptide 3,  $m/z$  7993.8, calcd 7991.3  $[\text{M} + \text{H}]^+$ . The amounts of the starting compounds and the generated products were quantified from the peak areas.

### Fluorescence Titration Analysis

Fluorescence spectra were recorded on a JASCO FP-750 spectrometer using a quartz cell. A stock solution of the probe

peptide was diluted with 50 mM HEPES buffer solution (pH 7.2, 100 mM NaCl) to prepare the solution with a final concentration (0.5  $\mu\text{M}$ ). The corresponding tag peptide solution was added dropwise to a 0.5  $\mu\text{M}$  of the probe peptide solution and the fluorescence spectra ( $\lambda_{\text{ex}} = 456$  nm) were measured at 25°C. An average value of three measurements was plotted as each point. Fluorescent titration curves ( $\lambda_{\text{em}} = 537$  nm for probe 1 and 2, 535 nm for probe 3, and 534 nm for probe 4 and 5) were analyzed with a nonlinear least-squares curve-fitting method to evaluate  $K_d$  values. For measurements of thermal denaturation, fluorescence spectra were recorded every 10°C from 4°C to 100°C after 10-min incubation of tag-probe pairs at each temperature. For measurements in thermal changes from high to low temperature, after 1-h incubation of tag-probe pairs at 100°C, fluorescence spectra were recorded every 10°C until 4°C.  $T_m$  values were estimated by a nonlinear least-squares curve-fitting method using GraphPad Prism 5 (MDF Co., Ltd.).

### Fluorescence Job's Titration

The fluorescent intensity at 505 nm was recorded on a JASCO FP-750 spectrometer using a quartz cell in 50 mM HEPES buffer (pH 7.2, 100 mM NaCl) at 25°C. The total concentration of the probe peptide and the tag peptide was fixed at 1.0  $\mu\text{M}$ . The concentrations of the tag peptide were 0, 0.2, 0.4, 0.5, 0.6, 0.8, and 1.0  $\mu\text{M}$ . This fluorescence Job's titration experiment clearly indicates that the probe peptide binds to the tag peptide in a 1:1 stoichiometry.

### CD Study

CD were recorded on a J-720WI spectropolarimeter using a quartz cell with 0.1 cm pathlength at 25°C. The stock solutions of tag-probe complexes were prepared and diluted with 50 mM Tris-HCl buffer solution (pH 7.2, 100 mM NaCl) to

prepare the solutions of a final concentration (1.0  $\mu$ M). Each spectrum shows an average value of three measurements. For measurements of thermal denaturation, CD spectra were recorded every 5°C from 4°C to 94°C after 10-min incubation of tag-probe pairs at each temperature. For measurements in thermal changes from high to low temperature, after 1-h incubation of tag-probe pairs at 94°C, CD spectra were recorded every 5°C until 4°C.

The authors deeply thank Prof. K. Akiyoshi (Tokyo Medical and Dental Univ.) for allowing access to a CD spectropolarimeter.

## REFERENCES

1. Terpe, K. *Appl Microbiol Biotechnol* 2003, 60, 523–533.
2. Hedhammar, M.; Gräslund, T.; Hober, S. *Chem Eng Technol* 2005, 28, 1315–1325.
3. Guignet, E. G.; Hovius, R.; Vogel, H. *Nat Biotechnol* 2004, 22, 440–444.
4. Goldsmith, C. R.; Jaworski, J.; Sheng, M.; Lippard, S. J. *J Am Chem Soc* 2006, 128, 418–419.
5. Hauser, C. T.; Tsien, R. Y. *Proc Natl Acad Sci USA* 2007, 104, 3693–3697.
6. Griffin, B. A.; Adams, S. R.; Tsien, R. Y. *Science* 1998, 281, 269–272.
7. Gaietta, G.; Deerinck, T. J.; Adams, S. R.; Bouwer, J.; Tour, O.; Laird, D. W.; Sosinsky, G. E.; Tsien, R. Y.; Ellisman, M. H. *Science* 2002, 296, 503–507.
8. Marks, K. M.; Rosinov, M.; Nolan, G. P. *Chem Biol* 2004, 11, 347–356.
9. Ojida, A.; Honda, K.; Shinmi, D.; Kiyonaka, S.; Mori, Y.; Hamachi, I. *J Am Chem Soc* 2006, 128, 10452–10459.
10. Chen, I.; Choi, Y.-A.; Ting, A. Y. *J Am Chem Soc* 2007, 129, 6619–6625.
11. O'Hare, H. M.; Johnsson, K.; Gautier, A. *Curr Opin Struct Biol* 2007, 17, 488–494.
12. Keppler, A.; Gendreizig, S.; Gronemeyer, T.; Pick, H.; Johnsson, K. *Nat Biotechnol* 2003, 21, 86–89.
13. Gautier, A.; Juillerat, A.; Heinis, C.; Correa, I. R., Jr.; Kindermann, M.; Beaufils, E.; Johnsson, K. *Chem Biol* 2008, 15, 128–136.
14. Yin, J.; Liu, F.; Li, X.; Walsh, C. T. *J Am Chem Soc* 2004, 126, 7754–7755.
15. Los, G. V.; Darzins, A.; Karassina, N.; Zimprich, C.; Learish, R.; McDougall, M. G.; Encell, L. P.; Friedman-Ohana, R.; Wood, M.; Vidurgiris, G.; Zimmerman, K.; Otto, P.; Klaubert, D. H.; Wood, K. V. *Promega Cell Notes* 2005, 11, 2–6.
16. Tripet, B.; Yu, L.; Bautista D. L.; Wong, W. Y.; Irvin, R. T.; Hodges, R. S. *Protein Eng* 1996, 9, 1029–1042.
17. Zhang, K.; Diehl, M. R.; Tirrell, D. A. *J Am Chem Soc* 2005, 127, 10136–10137.
18. Obataya, I.; Sakamoto, S.; Ueno, A.; Mihara, H. *Biopolymers* 2001, 59, 65–71.
19. Yadav, M. K.; Redman, J. E.; Leman, L. J.; Alvarez-Gutie'rrez, J. M.; Zhang, Y.; Stout, C. D.; Ghadiri, M. R. *Biochemistry* 2005, 44, 9723–9732.
20. Tsutsumi, H.; Nomura, W.; Abe, S.; Mino, T.; Masuda, A.; Ohashi, N.; Tanaka, T.; Ohba, K.; Yamamoto, N.; Akiyoshi, K.; Tamamura, H. *Angew Chem Int Ed* 2009, 48, 9164–9166.
21. Lovejoy, B.; Choe, S.; Cascio, D.; McRorie, D. K.; DeGrado, W. F.; Eisenberg, D. *Science* 1993, 259, 1288–1293.
22. Kuwabara, T.; Nakamura, A.; Ueno, A.; Toda, F. *J Phys Chem* 1994, 98, 6297–6303.
23. Ward, S. G.; Westwick, J. *Biochem J* 1998, 333, 457–470.
24. Tamamura, H.; Tsutsumi, H.; Nomura, W.; Tanaka, T.; Fujii, N. *Exp Opin Drug Disc* 2008, 3, 1155–1166.
25. Nomura, W.; Tanabe, Y.; Tsutsumi, H.; Tanaka, T.; Ohba, K.; Yamamoto, N.; Tamamura, H. *Bioconjugate Chem* 2008, 19, 1917–1920.
26. Chan, W. C.; White, P. D. In *Fmoc Solid Phase Peptide Synthesis: A Practical Approach*; Chan, W. C.; White, P. D., Eds.; Oxford University Press: New York, 2000; pp 41–76.
27. Dawson, P. E.; Muir, T.W.; Clark-Lewis, I.; Kent, S. B. H. *Science* 1994, 266, 776–779.
28. Muir, T. W.; Kent, S. B. H. *Annu Rev Biochem* 2000, 69, 923–960.
29. Nonaka, H.; Tsukiji, S.; Ojida, A.; Hamachi, I. *J Am Chem Soc* 2007, 129, 15777–15779.
30. Kamoto, M.; Umezawa, N.; Kato, N.; Higuchi, T. *Chem Eur J* 2008, 14, 8004–8012.
31. Bourel, L.; Carion, O.; Gras-Masse, H.; Melnyk, O. *J Peptide Sci* 2000, 6, 264–270.



## Peptide HIV-1 Integrase Inhibitors from HIV-1 Gene Products

Shintaro Suzuki,<sup>†,‡</sup> Emiko Urano,<sup>‡,‡</sup> Chie Hashimoto,<sup>†</sup> Hiroshi Tsutsumi,<sup>†</sup> Toru Nakahara,<sup>†</sup> Tomohiro Tanaka,<sup>†</sup> Yuta Nakanishi,<sup>†</sup> Kasthuraiah Maddali,<sup>§</sup> Yan Han,<sup>‡</sup> Makiko Hamatake,<sup>‡</sup> Kosuke Miyauchi,<sup>‡</sup> Yves Pommier,<sup>§</sup> John A. Beutler,<sup>⊥</sup> Wataru Sugiura,<sup>‡</sup> Hideyoshi Fuji,<sup>||</sup> Tyuji Hoshino,<sup>||</sup> Kyoko Itotani,<sup>†</sup> Wataru Nomura,<sup>†</sup> Tetsuo Narumi,<sup>†</sup> Naoki Yamamoto,<sup>‡</sup> Jun A. Komano,<sup>‡</sup> and Hirokazu Tamamura<sup>\*,†</sup>

<sup>†</sup>Department of Medicinal Chemistry, Institute of Biomaterials and Bioengineering, Tokyo Medical and Dental University, 2-3-10 Kandasurugadai, Chiyoda-ku, Tokyo 101-0062, Japan, <sup>‡</sup>AIDS Research Center, National Institute of Infectious Diseases, 1-23-1 Toyama, Shinjuku-ku, Tokyo 162-8640, Japan, <sup>§</sup>Laboratory of Molecular Pharmacology, Center for Cancer Research, National Cancer Institute, National Institutes of Health, Bethesda, Maryland 20892-4255, <sup>||</sup>Department of Physical Chemistry, Graduate School of Pharmaceutical Sciences, Chiba University, 1-33 Yayoi-cho, Inage-ku, Chiba 263-8522, Japan, and <sup>⊥</sup>Molecular Targets Laboratory, Center for Cancer Research, National Cancer Institute, National Institutes of Health, Frederick, Maryland 21702. <sup>#</sup> These authors contributed equally to this work.

Received March 17, 2010

Anti-HIV peptides with inhibitory activity against HIV-1 integrase (IN) have been found in overlapping peptide libraries derived from HIV-1 gene products. In a strand transfer assay using IN, inhibitory active peptides with certain sequential motifs related to Vpr- and Env-derived peptides were found. The addition of an octa-arginyl group to the inhibitory peptides caused a remarkable inhibition of the strand transfer and 3'-end-processing reactions catalyzed by IN and significant inhibition against HIV replication.

### Introduction

Many antiretroviral drugs are currently available to treat human immunodeficiency virus type 1 (HIV-1) infection. Viral enzymes such as reverse transcriptase (RT<sup>a</sup>), protease and integrase (IN), gp41, and coreceptors are the main targets for antiretroviral drugs that are under development. Because of the emergence of viral strains with multidrug resistance (MDR), however, new anti-HIV-1 drugs operating with different inhibitory mechanisms are required. Following the success of raltegravir, IN has emerged as a prime target. IN is an essential enzyme for the stable infection of host cells because it catalyzes the insertion of viral DNA inside the preintegration complex (PIC) into the genome of host cells in two successive reactions, designated as strand transfer and 3'-end-processing. It is assumed that the enzymatic activities of IN have to be negatively regulated in the PIC during its transfer from the cytoplasm to the nucleus. Otherwise, premature activation of IN can lead to the autointegration into the viral DNA itself, resulting in an aborted infection. We speculate that the virus, rather than the host cells, must encode a mechanism to prevent autointegration. The PIC contains in association with the viral nucleic acid, viral proteins such as RT, IN, capsids (p24<sup>CA</sup> and p7<sup>NC</sup>), matrix (p17<sup>MA</sup>), p6 and Vpr, cellular proteins HMG I (Y), and the barrier to autointegration factor (BAF).<sup>1–4</sup> It is likely that, due to their spatial proximity in the PIC, these proteins physically and functionally interact with each other. For instance, it is already known that RT activity inhibited by Vpr,<sup>5</sup> and that RT and IN inhibit each other.<sup>5–9</sup> Vpr also inhibits IN through its C-terminal domain.<sup>5,10</sup> Because these studies suggest that PIC components regulate each other's

function, we have attempted to obtain potent inhibitory lead compounds from a peptide fragment library derived from HIV-1 gene products, an approach which has been successful in finding a peptide IN inhibitor from LEDGF, a cellular IN binding protein.<sup>11</sup>

In this paper, we describe the screening of an overlapping peptide library derived from HIV-1 proteins, the identification of certain peptide motifs with inhibitory activity against HIV-1 IN, and the evaluation of effective inhibition of HIV-1 replication in cells using the identified peptide inhibitors possessing cell membrane permeability.

### Results and Discussion

An overlapping peptide library spanning HIV-1 SF2 *Gag*, *Pol*, *Vpr*, *Tat*, *Rev*, *Vpu*, *Env*, and *Nef*, provided by Dr. Iwamoto of the Institute of Medical Science at the University of Tokyo (Supporting Information, SI, Figure 2A), was screened with a strand transfer assay<sup>12</sup> in search of peptide pools with inhibitory activity against HIV-1 IN. The library consists of 658 peptide fragments derived from the HIV-1 gene products. Each peptide is composed of 10–17 amino acid residues with overlapping regions of 1–7 amino acid residues. Sixteen peptide pools containing between 16 and 65 peptides were used for the first screening at the final concentration of 5.0  $\mu$ M for each peptide (SI Figure 2B). This initial screening gave the results shown in Figure 1. Both Vpr and Env4 pools showed remarkable inhibition of IN strand transfer activity, and consequently a second screening was performed using the individual peptides contained in the Vpr and Env4 pools. A group of consecutive overlapping peptides in the Vpr pool (groups 13–15) and groups 4–6 and 20–21 in the Env4 pool were found to possess IN inhibitory activity (Figure 2). We focused on Vpr15 and Env4-4 peptides because they showed inhibitory activity against IN strand transfer reaction in a dose-dependent manner (Figure 3). The IC<sub>50</sub> values of Vpr15

\*To whom correspondence should be addressed. Phone: +81-3-5280-8036. Fax: +81-3-5280-8039. E-mail: tamamura.mr@tmd.ac.jp.

<sup>a</sup>Abbreviations: HIV, human immunodeficiency virus; IN, integrase; RT, reverse transcriptase; MDR, multidrug resistance; PIC, preintegration complex; BAF, barrier to autointegration factor; R<sub>8</sub>, octa-arginyl.



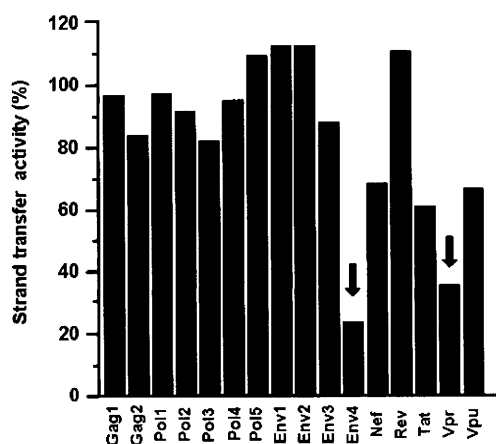


**Figure 1.** Inhibition of the IN strand transfer activity by peptide pools. Inhibition of the IN strand transfer activity was strongly inhibited by Env4 and Vpr pools (arrows). The y-axis represents the IN strand transfer activity relative to the solvent control (DMSO).

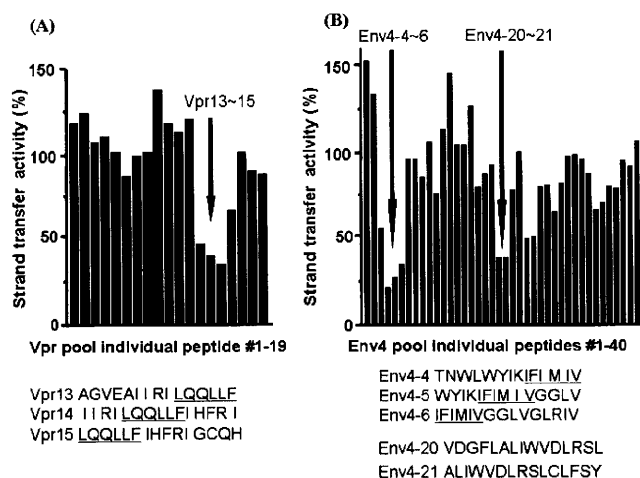


**Figure 2.** Identification of IN inhibitory peptides in the Vpr (A) and Env4 (B) pools based on the strand transfer activity of IN. The consecutive overlapping peptides display the inhibition of the strand transfer activity of IN (arrows). The y-axis represents the IN strand transfer activity relative to the solvent control (DMSO). The concentration of each peptide was  $5 \mu\text{M}$ . The common sequences of individual peptides derived from Vpr and Env4 pools with anti-IN activity are underlined.

and Env4-4 were estimated at  $5.5$  and  $1.9 \mu\text{M}$ , respectively. These peptides did not show any significant inhibitory activity against HIV-1 RT, suggesting that they might inhibit IN strand transfer reaction selectively.

The overlapping peptides of Vpr13-15 and Env4-4-6 have the common hexapeptide sequences LQQLLF and IFIMIV, respectively. The LQQLLF sequence covers positions 64–69 of Vpr, which is a part of the second helix of Vpr. The IFIMIV sequence corresponds to positions 684–689 of gp160, which is a part of the transmembrane domain of TM/gp41. These hexapeptides are thought to be critical to inhibition of IN activity. It was recently reported<sup>5</sup> that similar peptides derived from Vpr inhibit IN with  $\text{IC}_{50}$  values of  $1\text{--}16 \mu\text{M}$ , which is consistent with our data. In this report,<sup>5</sup> the peptide motif was found to be 15 amino acid residues spanning LQQLLF from the overlapping Vpr peptide library. In our study, more precise mapping of inhibitory motif in Vpr peptides was achieved by identifying the shorter effective peptide motif. We focused on the Vpr-derived peptide, LQQLLF (Vpr-1) to develop potent inhibitory peptides. However, the expression of inhibitory activity against IN

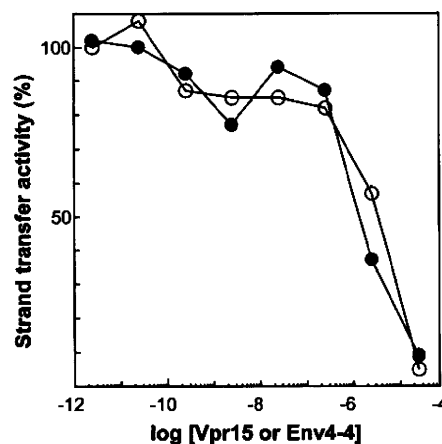


**Figure 3.** Concentration-dependent inhibition of IN strand transfer activities by Vpr15 (○) and Env4-4 (●) peptides. The y-axis represents the IN strand transfer activity relative to the solvent control (DMSO).

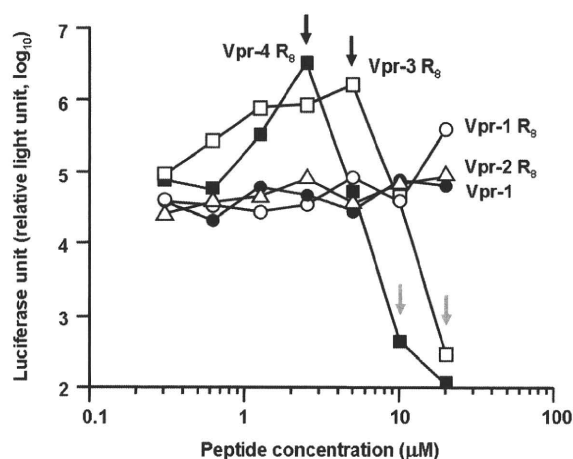
in vivo by only hexapeptides might be difficult because these hexapeptides penetrate the plasma membrane very poorly and to achieve antiviral activity, it is essential that they penetrate the cell membrane. To that effect, an octa-arginyl ( $\text{R}_8$ ) group<sup>13</sup> was fused to the Vpr-derived peptides (Table 1).  $\text{R}_8$  is a cell membrane permeable motif and its fusion with parent peptides successfully generates bioactive peptides without significant adverse effects or cytotoxicity.<sup>14–18</sup> In addition, the  $\text{R}_8$ -fusion could increase the solubility of Vpr-derived peptides which have a relatively hydrophobic character.

The inhibitory activity of Vpr-1 and Vpr-1-4  $\text{R}_8$  peptides against IN was evaluated based on the strand transfer and 3'-end-processing reactions in vitro (Table 1).<sup>19,20</sup> Vpr-1 did not show strong inhibition of either IN activity, but the  $\text{IC}_{50}$  of Vpr-1  $\text{R}_8$  toward the strand transfer reaction of IN was 10-fold lower than that of Vpr-1 lacking the  $\text{R}_8$  group. This indicates that the positive charges derived from the  $\text{R}_8$  group might enhance the inhibitory activity of the Vpr-1 peptide. Because we were concerned that the strong positive charges close to the LQQLLF motif might interfere with the inhibitory activity, the 6 amino acid sequence (–IHFRIG–) was inserted as a spacer between LQQLLF and  $\text{R}_8$  (Vpr-3  $\text{R}_8$ ). The IHFRIG sequence was used to reconstitute the natural Vpr. The  $\text{IC}_{50}$  values of Vpr-2  $\text{R}_8$  for the strand transfer and 3'-end-processing activities of IN were  $0.70$  and  $0.83 \mu\text{M}$ , respectively, while Vpr-3  $\text{R}_8$  showed potent IN inhibitory activities of  $4.0$  and  $8.0 \text{ nM}$  against the strand transfer and 3'-end-processing activities, respectively. This result indicates the additional importance of the IHFRIG sequence for inhibitory activities against IN. The increased IN inhibitory activities might be achieved presumably by the synergistic effect of the LQQLLF motif, the IHFRIG sequence, and the  $\text{R}_8$  group. Vpr-4  $\text{R}_8$ , in which the EAIIRI sequence was attached to further reconstitute the Vpr helix 2, showed inhibitory activities similar to those of Vpr-3  $\text{R}_8$ , suggesting that reconstitution of helix 2 of Vpr is not necessary for efficient IN inhibition. Vpr-3  $\text{R}_8$  and Vpr-4  $\text{R}_8$ , with  $\text{IC}_{50} > 0.5 \mu\text{M}$ ,<sup>21</sup> were less potent inhibitors of RT-associated RNase H activity, indicating that these peptides can selectively inhibit IN. These results suggest that Vpr-derived peptides are novel and distinct from any other IN inhibitors reported to date.

For rapid assessment of the antiviral effect of Vpr-derived peptides, we established an MT-4 Luc system in which MT-4 cells were stably transduced with the firefly luciferase expression cassette by a murine leukemia viral vector (SI Figure 3).

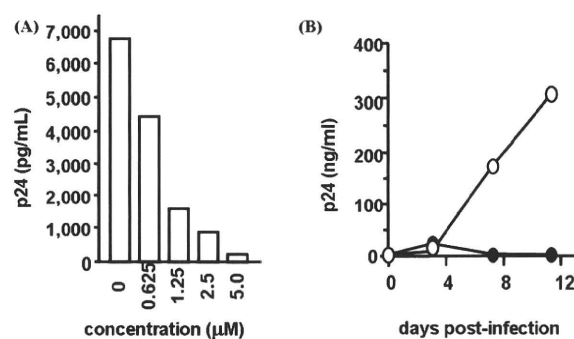
**Table 1.** Sequences of Vpr-Derived Peptides and Their IC<sub>50</sub> Values toward the Strand Transfer and 3'-End Processing Reactions of IN

		IC <sub>50</sub> (μM)	
		strand transfer	3'-end processing
Vpr-1	LQQLLF	68 ± 1.0	> 100
Vpr-1 R <sub>8</sub>	Ac-LQQLLF -RRRRRRRRR-NH <sub>2</sub>	6.1 ± 1.1	> 11
Vpr-2 R <sub>8</sub>	Ac-IHFRIG-RRRRRRRRR-NH <sub>2</sub>	0.70 ± 0.06	0.83 ± 0.07
Vpr-3 R <sub>8</sub>	Ac-LQQLLF IHFRIG-RRRRRRRRR-NH <sub>2</sub>	0.004 ± 0.0001	0.008 ± 0.001
Vpr-4 R <sub>8</sub>	Ac-EAIIIR LQQLLF IHFRIG-RRRRRRRRR-NH <sub>2</sub>	0.005 ± 0.002	0.006 ± 0.006

**Figure 4.** Luciferase signals in MT-4 Luc cells infected with HIV-1 in the presence of various concentrations of Vpr-derived peptides: Vpr-1 (●), Vpr-1 R<sub>8</sub> (○), Vpr-2 R<sub>8</sub> (△), Vpr-3 R<sub>8</sub> (□), Vpr-4 R<sub>8</sub> (■).

MT-4 Luc cells constitutively express high levels of luciferase which are significantly reduced by HIV-1 infection due to their high susceptibility to cell death upon HIV-1 infection. Protection of MT-4 Luc cells from HIV-1-induced cell death maintains the luciferase signals at high levels. In addition, the cytotoxicity of Vpr-derived peptides can be evaluated by a decrease of luciferase signals in these MT-4 Luc systems. Vpr-2 R<sub>8</sub>, which is a weak IN inhibitor, showed no significant anti-HIV-1 activity below concentrations of 20 μM, suggesting that its moderate IC<sub>50</sub> level in vitro is not sufficient to suppress HIV-1 replication in tissue culture and that the R<sub>8</sub> group is not significantly cytotoxic (Figure 4). Vpr-1 did not show any inhibitory effects against HIV-1 replication; however, Vpr-1 R<sub>8</sub> displayed a weak antiviral effect at a concentration of 20 μM and both Vpr-3 R<sub>8</sub> and Vpr-4 R<sub>8</sub> showed significant inhibitory effects against HIV-1 replication. The R<sub>8</sub> peptide did not show significant anti-HIV activity (IC<sub>50</sub> > 50 μM, data not shown). These results suggest that the addition of the R<sub>8</sub> group enables Vpr-derived peptides to enter the cytoplasm and access IN, with the result that HIV-1 replication could be effectively inhibited.

Because Vpr-3 R<sub>8</sub> was less cytotoxic than Vpr-4 R<sub>8</sub>, the inhibitory activities of Vpr-3 R<sub>8</sub> were further investigated. Two replication assay systems, R5-tropic HIV-1<sub>JR-CSF</sub> on NP2-CD4-CCR5 cells and X4-tropic HIV-1<sub>HXB2</sub> on MT-4 cells, were utilized. NP2-CD4-CCR5 cells were infected with HIV-1<sub>JR-CSF</sub> in the presence of various concentrations of Vpr-3 R<sub>8</sub>. On day 4 postinfection, the culture supernatant was collected and the concentration of viral p24 antigen was measured by an ELISA assay. The p24 levels decreased in a dose-dependent manner with increasing the concentration of Vpr-3 R<sub>8</sub>; 50% inhibition of p24 expression was obtained with approximately 0.8 μM of Vpr-3 R<sub>8</sub> (Figure 5A). This concentration was approximately 10-fold lower than the concentration of Vpr-3 R<sub>8</sub> known to be cytotoxic (Figure 4). Second, MT-4 cells were infected with HIV-1<sub>HXB2</sub> and the replication kinetics was monitored in the

**Figure 5.** (A) The inhibition of HIV-1<sub>JR-CSF</sub> replication in NP2-CD4-CCR5 cells in the presence of various concentrations of Vpr-3 R<sub>8</sub>. (B) The replication kinetics of HIV-1<sub>HXB2</sub> in MT-4 cells in the presence of Vpr-3 R<sub>8</sub> (●). The concentration of Vpr-3 R<sub>8</sub> was fixed at 0.5 μM. Absence of Vpr-3 R<sub>8</sub> (○).

presence of 0.5 μM Vpr-3 R<sub>8</sub>. The degree of replication of HIV-1<sub>HXB2</sub> was quite low in the presence of Vpr-3 R<sub>8</sub>, while replication of HIV-1<sub>HXB2</sub> was robust in the absence of Vpr-3 R<sub>8</sub> (Figure 5B), suggesting that Vpr-3 R<sub>8</sub> strongly suppresses the replication of HIV-1 in cells. To examine whether the HIV-1 replication was blocked through the inhibition of IN activity, quantitative real-time PCR was performed. If IN is inhibited, the efficiency of viral genome integration should be decreased while the reverse transcription of viral genome should not be affected. Accordingly, NP2-CD4-CXCR4 cells were infected with HIV-1<sub>HXB2</sub> in the presence or absence of 0.5 μM Vpr-3 R<sub>8</sub>. Genomic DNA was extracted on day 2 postinfection, and the viral DNA was quantified at the various steps of viral entry phase. The level of “strong stop DNA”, representing the total genome of infected virus in Vpr-3 R<sub>8</sub>-treated cells, was similar (139.7%) to that in DMSO-treated control cells and the level of viral DNA generated at the late stage of reverse transcription in Vpr-3 R<sub>8</sub>-treated cells was slightly decreased (84.4%) compared to control cells. This small decline can probably be attributed to the weak anti-RNase H activity of Vpr-3 R<sub>8</sub>. On the other hand, a drastic decrease of Alu-LTR products was observed in Vpr-3 R<sub>8</sub>-treated cells (15.8%), indicating an inhibition of integrated viral genome. Concomitantly, the double LTR products, representing the end-joined viral genome catalyzed by host cellular enzymes, were increased by a factor of 8 (779.8%). These results strongly suggest that Vpr-3 R<sub>8</sub> blocks viral infection by inhibiting IN activity in cells, consistent with our in vitro observations. Judging by these results, Vpr-derived peptides with the R<sub>8</sub> group are potent IN inhibitors that suppress HIV-1 replication in vivo.

Finally, in silico molecular docking simulations of Vpr-derived peptides and HIV-1 IN were performed. The Vpr-derived peptides are located in the second helix of Vpr and were thus considered to have an α-helical conformation.<sup>22</sup> Docking simulations of three peptides (Vpr13, Vpr14, and Vpr15), using the predicted structure of the HIV-1 IN dimer as a template,<sup>23</sup> were performed by GOLD software to investigate the binding mode of the peptides, the binding affinity of



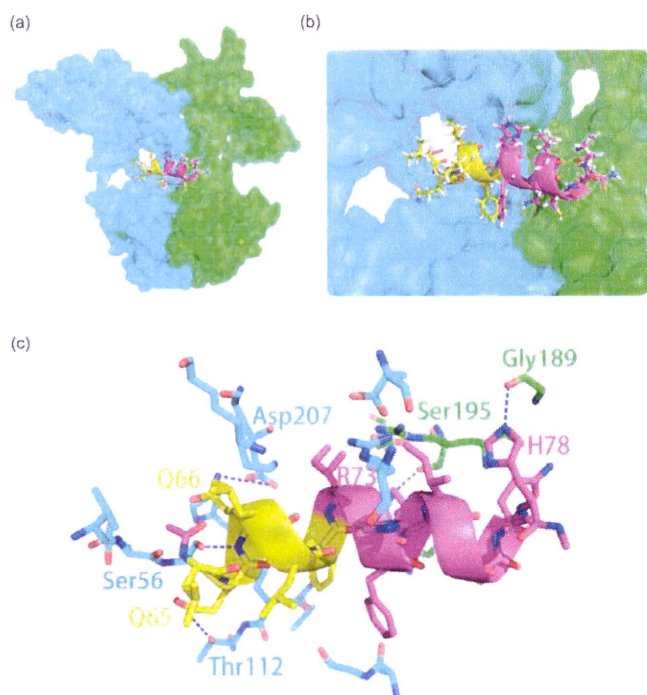


**Figure 6.** Predicted binding mode of Vpr15 to HIV-1 IN by GOLD. An overall view of (a) the complex obtained by docking Vpr15 with the HIV-1 IN dimer and (b) the closer view of the complex. The predicted structure of full-length HIV-1 IN was used as a template. Each HIV-1 IN monomer was shown as green or cyan surface. The docked Vpr15 is shown as a cartoon. The yellow-colored region is the LQQLLF motif. The GOLD score representing the docking complementarity is 69.83, indicating the high binding affinity between Vpr15 and IN. The hydrogen-bond interactions between HIV-1 IN and Vpr15 were presented by LIGPLOT software shown as blue dotted line (c).

the peptides being evaluated by GOLD Fitness score. The predicted binding mode of Vpr15 to IN is shown in Figure 6. Our results predict that the three Vpr-derived peptides interact with the cleft between the amino-terminal domain and the core domain of HIV-1 IN. This region is distinct from the nucleic acid interacting surfaces, indicating that the Vpr-derived peptides inhibit IN function in an allosteric manner. A previous report provided a model in which a Vpr peptide was bound to IN in a manner similar with our model<sup>5</sup> and, interestingly, the peptides were bound to IN with an exterior surface of Vpr. This earlier report that the full-length Vpr inhibits IN<sup>10</sup> strongly supports the predicted binding mode of Vpr15. Five hydrogen-bond interactions between HIV-1 IN and Vpr15 were identified by LIGPLOT analysis,<sup>24</sup> which invoked the following IN-Vpr amino acids: IN Thr112-Vpr Gln65, IN Ser56-Vpr Gln66, IN Asp207-Vpr Gln66, IN Ser195-Vpr Arg73, and IN Gly189-Vpr His78. The numbering of Vpr amino acids is based on the Vpr full-length coordinate, Figure 6. Additional hydrophobic contacts between IN and Vpr15 were found in which the following IN-Vpr amino acid pairs are involved: IN Lys211-Vpr Gln66, IN Pro109-Vpr Phe69, IN Arg262-Vpr His71, and IN Arg187-Vpr Gln77. These data indicate that the Gln65, Gln66, and Phe69 residues in Vpr-derived peptides play a major role in the interaction between IN and Vpr-derived peptides.

## Conclusions

In summary, two peptide motifs, LQQLLF from Vpr and IFIMIV from Env4, possessing inhibitory activity against

HIV-1 IN, were identified through the screening of overlapping peptide library derived from HIV-1 gene products. We initially speculate that HIV encodes a mechanism to prevent autointegration in the PIC because integration activity must be regulated until the virus infects cells. This speculation is supported by the finding that IN inhibitors exist in the viral PIC components. Vpr-derived peptides with the R<sub>8</sub> group showed remarkable inhibitory activities against the strand transfer and 3'-end-processing reactions catalyzed by HIV-1 IN *in vitro*. In addition, Vpr-3 R<sub>8</sub> and Vpr-4 R<sub>8</sub> were shown to inhibit HIV-1 replication with submicromolar IC<sub>50</sub> values in cells using the MT-4 Luc cell system. In the quantitative analysis of p24 antigen, 50% inhibition of HIV-1<sub>JR-CSF</sub> replication was caused by approximately 0.8 μM of Vpr-3 R<sub>8</sub>, and the replication of HIV-1<sub>HXB2</sub> was extensively suppressed in the long term by Vpr-3 R<sub>8</sub> at 0.5 μM concentrations. Our finding suggest that these peptides could serve as lead compounds for novel IN inhibitors. Amino acid residues critical to the interaction of Vpr-derived peptides with IN were identified by our *in silico* molecular docking simulations, and suggests that more potent peptides<sup>25</sup> or peptidomimetic IN inhibitors represent a novel avenue for future small molecule inhibitors of IN and HIV integration.

## Experimental Section

**Peptide Synthesis.** Vpr-derived peptides containing the R<sub>8</sub> group were synthesized by stepwise elongation techniques of Fmoc-protected amino acids on NovaSyn TGR resin. Coupling reactions were performed using 5.0 equiv of Fmoc-protected amino acid, 5.0 equiv of diisopropylcarbodiimide, and 5.0 equiv of 1-hydroxybenzotriazole monohydrate. Cleavage of peptides from resin and side chain deprotection were carried out with 10 mL of TFA in the presence of 0.25 mL of *m*-cresol, 0.75 mL of thioanisole, 0.75 mL of 1,2-ethanedithiol, and 0.1 mL of water as scavenger by stirring for 1.5 h. After filtration of the deprotected peptides, the filtrate was concentrated under reduced pressure, and crude peptides were precipitated in cooled diethyl-ether. All crude peptides were purified by RP-HPLC and identified by MALDI-TOFMS. Purities of all final compounds were confirmed (>95% purity) by analytical HPLC. Detailed data are provided in SI.

**Enzyme Assays.** The strand transfer assay for the first screening was performed as described previously.<sup>12</sup> The IN strand transfer and 3'-end-processing assays for peptide motif characterizations were performed as described previously.<sup>19,20</sup> RNase H activity was measured as described by Beutler et al.<sup>21</sup>

**Replication Assays.** For HIV-1 replication assays, 1 × 10<sup>5</sup> cells were incubated at room temperature for 30 min with an HIV-1 containing culture supernatant (ca. 0.2–50 ng p24) and then washed and incubated. Culture supernatants were collected at different time points, and then the cells were passaged if necessary. Levels of p24 antigen were measured using a Retro TEK p24 antigen ELISA kit, according to the manufacture's protocol. Signals were detected using an ELx808 microplate photometer.

For MT-4 Luc assays, MT-4 Luc cells (1 × 10<sup>3</sup> cells) grown in 96-well plates were infected with HIV-1<sub>XHB2</sub> (ca. 0.2–10 ng p24) in the presence of varying concentrations of Vpr-3 R<sub>8</sub>. At 6–7 d postinfection, cells were lysed and luciferase activity was measured using the Steady-Glo assay kits according to the manufacture's protocol. Chemiluminescence was detected with a Veritas luminometer.

**Acknowledgment.** We thank Prof. A. Iwamoto's group of the Institute of Medical Science at the University of Tokyo for the peptide libraries and Dr. M. Nicklaus from NCI/NIH for providing the modeled structure of full-length HIV-1 IN. T.T. is supported by JSPS research fellowships for young scientists.

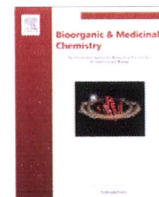
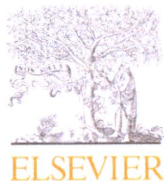
This work was supported in part by Grant-in-Aid for Scientific Research from the Ministry of Education, Culture, Sports, Science, and Technology of Japan, and Health and Labor Sciences Research Grants from Japanese Ministry of Health, Labor, and Welfare. K.M. and Y.P. are supported by the Intramural Program of the National Cancer Institute, Center for Cancer Research.

**Supporting Information Available:** Additional experimental procedures including MS data and figures; HPLC charts of final compounds, explanation for HIV-1 genes and the peptide pools, and illustration of MT-4 Luc system. This material is available free of charge via the Internet at <http://pubs.acs.org>.

## References

- (1) Bukrinsky, M. I.; Haggerty, S.; Dempsey, M. P.; Sharova, N.; Adzhubei, A.; Spitz, L.; Lewis, P.; Goldfarb, D.; Emerman, M.; Stevenson, M. A nuclear-localization signal within HIV-1 matrix protein that governs infection of nondividing cells. *Nature* **1993**, *365*, 666–669.
- (2) Miller, M. D.; Farnet, C. M.; Bushman, F. D. Human immunodeficiency virus type 1 preintegration complexes: studies of organization and composition. *J. Virol.* **1997**, *71*, 5382–5390.
- (3) Farnet, C. M.; Bushman, F. D. HIV-1 cDNA integration: Requirement of HMG I(Y) protein for function of preintegration complexes in vitro. *Cell* **1997**, *88*, 483–492.
- (4) Chen, H.; Engelman, A. The barrier-to-autointegration protein is a host factor for HIV type 1 integration. *Proc. Natl. Acad. Sci. U.S.A.* **1998**, *95*, 15270–15274.
- (5) Gleenberg, I. O.; Herschhorn, A.; Hizi, A. Inhibition of the activities of reverse transcriptase and integrase of human immunodeficiency virus type-1 by peptides derived from the homologous viral protein R (Vpr). *J. Mol. Biol.* **2007**, *369*, 1230–1243.
- (6) Gleenberg, I. O.; Avidan, O.; Goldgur, Y.; Herschhorn, A.; Hizi, A. Peptides derived from the reverse transcriptase of human immunodeficiency virus type 1 as novel inhibitors of the viral integrase. *J. Biol. Chem.* **2005**, *280*, 21987–21996.
- (7) Hehl, E. A.; Joshi, P.; Kalpana, G. V.; Prasad, V. R. Interaction between human immunodeficiency virus type 1 reverse transcriptase and integrase proteins. *J. Virol.* **2004**, *78*, 5056–5067.
- (8) Tasara, T.; Maga, G.; Hottiger, M. O.; Hubscher, U. HIV-1 reverse transcriptase and integrase enzymes physically interact and inhibit each other. *FEBS Lett.* **2001**, *507*, 39–44.
- (9) Gleenberg, I. O.; Herschhorn, A.; Goldgur, Y.; Hizi, A. Inhibition of human immunodeficiency virus type-1 reverse transcriptase by a novel peptide derived from the viral integrase. *Arch. Biochem. Biophys.* **2007**, *458*, 202–212.
- (10) Bischerour, J.; Tauc, P.; Leh, H.; De Rocquigny, H.; Roques, B.; Mouscadet, J. F. The (52–96) C-Terminal domain of Vpr stimulates HIV-1 IN-mediated homologous strand transfer of mini-viral DNA. *Nucleic Acids Res.* **2003**, *31*, 2694–2702.
- (11) Hayouka, Z.; Rosenbluh, J.; Levin, A.; Loya, S.; Lebendiker, M.; Vepintsev, D.; Kotler, M.; Hizi, A.; Loyter, A.; Friedler, A. Inhibiting HIV-1 integrase by shifting its oligomerization equilibrium. *Proc. Natl. Acad. Sci. U.S.A.* **2007**, *104*, 8316–8312.
- (12) Yan, H.; Mizutani, T. C.; Nomura, N.; Tanaka, T.; Kitamura, Y.; Miura, H.; Nishizawa, M.; Tatsumi, M.; Yamamoto, N.; Sugiura, W. A novel small molecular weight compound with a carbazole structure that demonstrates potent human immunodeficiency virus type-1 integrase inhibitory activity. *Antivir. Chem. Chemother.* **2005**, *16*, 363–373.
- (13) Suzuki, T.; Futaki, S.; Niwa, M.; Tanaka, S.; Ueda, K.; Sugiura, Y. Possible existence of common internalization mechanisms among arginine-rich peptides. *J. Biol. Chem.* **2002**, *277*, 2437–2443.
- (14) Wender, P. A.; Mitchell, D. J.; Pattabiraman, K.; Pelkey, E. T.; Steinman, L.; Rothbard, J. B. The design, synthesis, and evaluation of molecules that enable or enhance cellular uptake: Peptoid molecular transporters. *Proc. Natl. Acad. Sci. U.S.A.* **2000**, *97*, 13003–13008.
- (15) Matsushita, M.; Tomizawa, K.; Moriwaki, A.; Li, S. T.; Terada, H.; Matsui, H. A high-efficiency protein transduction system demonstrating the role of PKA in long-lasting long-term potentiation. *J. Neurosci.* **2001**, *21*, 6000–6007.
- (16) Takenobu, T.; Tomizawa, K.; Matsushita, M.; Li, S. T.; Moriwaki, A.; Lu, Y. F.; Matsui, H. Development of p53 protein transduction therapy using membrane-permeable peptides and the application to oral cancer cells. *Mol. Cancer Ther.* **2002**, *1*, 1043–1049.
- (17) Wu, H. Y.; Tomizawa, K.; Matsushita, M.; Lu, Y. F.; Li, S. T.; Matsui, H. Poly-arginine-fused calpastatin peptide, a living cell membrane-permeable and specific inhibitor for calpain. *Neurosci. Res.* **2003**, *47*, 131–135.
- (18) Rothbard, J. B.; Garlington, S.; Lin, Q.; Kirschberg, T.; Kreider, E.; McGrane, P. L.; Wender, P. A.; Khavari, P. A. Conjugation of arginine oligomers to cyclosporin A facilitates topical delivery and inhibition of inflammation. *Nature Med.* **2000**, *6*, 1253–1257.
- (19) Marchand, C.; Zhang, X.; Pais, G. C. G.; Cowansage, K.; Neamati, N.; Burke, T. R., Jr.; Pommier, Y. Structural determinants for HIV-1 integrase inhibition by beta-diketo acids. *J. Biol. Chem.* **2002**, *277*, 12596–12603.
- (20) Semenova, E. A.; Johnson, A. A.; Marchand, C.; Davis, D. A.; Tarchoan, R.; Pommier, Y. Preferential inhibition of the magnesium-dependent strand transfer reaction of HIV-1 integrase by alpha-hydroxytropolones. *Mol. Pharmacol.* **2006**, *69*, 1454–1460.
- (21) Parniak, M. A.; Min, K. L.; Budihas, S. R.; Le Grice, S. F. J.; Beutler, J. A. A fluorescence-based high-throughput screening assay for inhibitors of HIV-1 reverse transcriptase associated ribonuclease H activity. *Anal. Biochem.* **2003**, *322*, 33–39.
- (22) Morellet, N.; Bouaziz, S.; Petitjean, P.; Roques, B. P. NMR structure of the HIV-1 regulatory protein Vpr. *J. Mol. Biol.* **2003**, *327*, 215–227.
- (23) Karki, R. G.; Tang, Y.; Burke, T. R., Jr.; Nicklaus, M. C. Model of full-length HIV-1 integrase complexed with viral DNA as template for anti-HIV drug design. *J. Comput.-Aided Mol. Des.* **2004**, *18*, 739–760.
- (24) Wallace, A. C.; Laskowski, R. A.; Thornton, J. M. LIGPLOT—a program to generate schematic diagrams of protein ligand interactions. *Protein Eng.* **1995**, *8*, 127–134.
- (25) Li, H.-Y.; Zawahir, Z.; Song, L.-D.; Long, Y.-Q.; Neamati, N. Sequence-based design and discovery of peptide inhibitors of HIV-1 integrase: insight into the binding mode of the enzyme. *J. Med. Chem.* **2006**, *49*, 4477–4486.





## Peptidic HIV integrase inhibitors derived from HIV gene products: Structure–activity relationship studies

Shintaro Suzuki<sup>a</sup>, Kasthuraiah Maddali<sup>b</sup>, Chie Hashimoto<sup>a</sup>, Emiko Urano<sup>c</sup>, Nami Ohashi<sup>a</sup>, Tomohiro Tanaka<sup>a</sup>, Taro Ozaki<sup>a</sup>, Hiroshi Arai<sup>a</sup>, Hiroshi Tsutsumi<sup>a</sup>, Tetsuo Narumi<sup>a</sup>, Wataru Nomura<sup>a</sup>, Naoki Yamamoto<sup>c,d</sup>, Yves Pommier<sup>b</sup>, Jun A. Komano<sup>c</sup>, Hirokazu Tamamura<sup>a,\*</sup>

<sup>a</sup> Institute of Biomaterials and Bioengineering, Tokyo Medical and Dental University, Chiyoda-ku, Tokyo 101-0062, Japan

<sup>b</sup> Laboratory of Molecular Pharmacology, Center for Cancer Research, National Cancer Institute, National Institutes of Health, Bethesda, MD 20892-4255, USA

<sup>c</sup> AIDS Research Center, National Institute of Infectious Diseases, Shinjuku-ku, Tokyo 162-8640, Japan

<sup>d</sup> Department of Microbiology, Yong Loo Lin School of Medicine, National University of Singapore, Singapore 117597, Singapore

### ARTICLE INFO

#### Article history:

Received 28 June 2010

Revised 17 July 2010

Accepted 20 July 2010

Available online 25 July 2010

#### Keywords:

HIV integrase  
Inhibitory peptide  
Glu-Lys pairs  
Ala-scan

### ABSTRACT

Structure–activity relationship studies were conducted on HIV integrase (IN) inhibitory peptides which were found by the screening of an overlapping peptide library derived from HIV-1 gene products. Since these peptides located in the second helix of Vpr are considered to have an  $\alpha$ -helical conformation, Glu-Lys pairs were introduced into the *i* and *i* + 4 positions to increase the helicity of the lead compound possessing an octa-arginyl group. Ala-scan was also performed on the lead compound for the identification of the amino acid residues responsible for the inhibitory activity. The results indicated the importance of an  $\alpha$ -helical structure for the expression of inhibitory activity, and presented a binding model of integrase and the lead compound.

© 2010 Elsevier Ltd. All rights reserved.

### 1. Introduction

Highly active anti-retroviral therapy (HAART), which involves a combination of two or three agents from two categories, reverse transcriptase inhibitors and protease inhibitors, has brought us remarkable success in the clinical treatment of HIV-infected and AIDS patients.<sup>1</sup> However, it has been accompanied by serious clinical problems including the emergence of viral strains with multi-drug resistance (MDR), considerable adverse effects and nonetheless high costs. As a result, new categories of anti-HIV agents operating with mechanisms of action different from those of the above inhibitors are sought. HIV-1 integrase (IN) is a critical enzyme for the stable infection of host cells since it catalyzes the insertion of viral DNA into the genome of host cells, by means of strand transfer and 3'-end processing reactions and thus it is an attractive target for the development of anti-HIV agents. Recently, the first IN inhibitor, raltegravir (Merck),<sup>2</sup> has appeared in a clinical setting. It is assumed that the activity of IN must be negatively regulated during the translocation of the viral DNA from the cytoplasm to the nucleus to prevent auto-integration. The virus, as well as the host cells, must encode mechanism(s) to prevent auto-integration since

the regulation of IN activity is critical for the virus to infect cells.<sup>3</sup> By screening a library of overlapping peptides derived from HIV-1 SF2 gene products we have found three Vpr-derived peptides, **1**, **2** and **3**, which possess significant IN inhibitory activity, indicating that IN inhibitors exist in the viral pre-integration complex (PIC).<sup>4</sup> The above inhibitory peptides, **1**, **2** and **3**, are consecutive overlapping peptides (Fig. 1). Compounds **4** and **5** are 12- and 18-mers from the original Vpr-sequence with the addition of an octa-arginyl group<sup>5</sup> into the C-terminus for cell membrane permeability, respectively. Compounds **4** and **5** have IN inhibitory activity and anti-HIV activity. Here, we report structure–activity relationship studies on these lead compounds for the development of more potent IN inhibitors.

### 2. Results and discussion

To determine which lead compound is most suitable for further experiments, five peptides **6–10**, which were elongated by one amino acid starting with compound **4** and extended ultimately to **5**, were synthesized (Fig. 2). Judging by the 3'-end processing and strand transfer reactions *in vitro*,<sup>6</sup> these peptides **4–10** had similar inhibitory potencies (Table 1). As a result, we concluded that 12 amino acid residues derived from the original Vpr-sequence are of sufficient for IN inhibitory activity, and any peptide among **4–10** is a suitable lead.

\* Corresponding author.

E-mail address: [tamamura.mr@tmd.ac.jp](mailto:tamura.mr@tmd.ac.jp) (H. Tamamura).



- 1 AGVEAIIRILQQLLF  
 2 IIRILQQLLFHFRI  
 3 LQQLLFHFRIKGCQH  
 4 Ac-LQQLLFHFRIK-RRRRRRRR-NH<sub>2</sub>  
 5 Ac-EAIIRILQQLLFHFRIK-RRRRRRRR-NH<sub>2</sub>

**Figure 1.** Amino acid sequences of compounds 1–5. Compounds 1–3 are consecutive overlapping peptides with free N-/C-terminus. These were found by the IN inhibitory screening of a peptide library derived from HIV-1 gene products. Compounds 4 and 5 are cell penetrative leads of IN inhibitors.

- 4 Ac-LQQLLFHFRIK-RRRRRRRR-NH<sub>2</sub>  
 6 Ac-ILQQLLFHFRIK-RRRRRRRR-NH<sub>2</sub>  
 7 Ac-RILQQLLFHFRIK-RRRRRRRR-NH<sub>2</sub>  
 8 Ac-IRILQQLLFHFRIK-RRRRRRRR-NH<sub>2</sub>  
 9 Ac-IIRILQQLLFHFRIK-RRRRRRRR-NH<sub>2</sub>  
 10 Ac-AIIRILQQLLFHFRIK-RRRRRRRR-NH<sub>2</sub>  
 5 Ac-EAIIRILQQLLFHFRIK-RRRRRRRR-NH<sub>2</sub>

**Figure 2.** Amino acid sequences of compounds 6–10, which are elongated by one amino acid from compound 4 to 5.

**Table 1**

IC<sub>50</sub> values of compounds 4–10 toward the 3'-end processing and strand transfer reactions catalyzed by HIV-1 IN

Compound	IC <sub>50</sub> (μM)	
	3'-End processing	Strand transfer
4	0.13 ± 0.02	0.06 ± 0.01
5	0.09 ± 0.01	0.04 ± 0.01
6	0.10 ± 0.01	0.07 ± 0.01
7	0.13 ± 0.02	0.11 ± 0.01
8	0.26 ± 0.04	0.11 ± 0.03
9	0.11 ± 0.01	0.07 ± 0.01
10	0.08 ± 0.01	0.05 ± 0.01

Structural analysis showed that the Vpr-derived peptides, 1, 2 and 3, are located in the second helix of Vpr and were thus considered to have an α-helical conformation.<sup>7</sup> Compound 5 was adopted as a lead for the development of compounds with an increase in α-helicity since a longer peptide is likely to form a more stable α-helical structure than a shorter one. Initially, Glu (E) and Lys (K) were introduced in pairs into compound 5 at the *i* and *i*+4 positions. In general, such disposition of Glu-Lys pairs at *i* and *i*+4 positions is considered to cause an increase in α-helicity due to formation of an ionic interaction of a β-carboxy group of Glu and an ε-amino group of Lys. Several analogs of 5 with Glu-Lys pairs were synthesized by Fmoc-solid phase peptide synthesis (Fig. 3). In the inhibitory assay against the 3'-end processing and strand transfer reactions catalyzed by HIV-1 IN in vitro, compounds 11 and 15 showed more potent inhibitory activities than 5 (Table 2). Substitution of Glu-Lys for His<sup>14</sup>-Gly<sup>18</sup> or Ile<sup>3</sup>-Leu<sup>7</sup> caused no decrease in IN inhibitory activity but a significant increase in activity, suggesting that Ile<sup>3</sup>, Leu<sup>7</sup>, His<sup>14</sup> and Gly<sup>18</sup> are not indispensable for activity. Substitution of Glu-Lys for Ala<sup>2</sup>-Ile<sup>6</sup> or Gln<sup>9</sup>-Ile<sup>13</sup> caused a slight decrease in IN inhibitory activity against the 3'-end processing and strand transfer reactions (compounds 12 and 13), indicating that Ala<sup>2</sup> and/or Ile<sup>6</sup>, and Gln<sup>9</sup> and/or Ile<sup>13</sup> are partly required for activity. Substitution of Glu-Lys for Ile<sup>4</sup>-Gln<sup>8</sup> caused a 2–4-fold decrease in IN inhibitory activity against the 3'-end processing and strand transfer reactions (compound 14), showing that Ile<sup>4</sup> and/or Gln<sup>8</sup> are essential for activity. Substitution of Glu-Lys for Leu<sup>11</sup>-Phe<sup>15</sup> caused an eightfold decrease in IN inhibitory activity against the 3'-end processing reaction and a 1.5-fold decrease in IN inhibitory activity against the

- 1 5 10 15  
 5 Ac-EAIIRILQQLLFHFRIK-RRRRRRRR-NH<sub>2</sub>  
 11 Ac-EAIIRILQQLLFHFRIK-RRRRRRRR-NH<sub>2</sub>  
 12 Ac-EEIIRKLLQQLLFHFRIK-RRRRRRRR-NH<sub>2</sub>  
 13 Ac-EAIIRILQQLLFHFRIK-RRRRRRRR-NH<sub>2</sub>  
 14 Ac-EAIIRILQQLLFHFRIK-RRRRRRRR-NH<sub>2</sub>  
 15 Ac-EAEIRIKQQLLFHFRIK-RRRRRRRR-NH<sub>2</sub>  
 16 Ac-EAIIRILQQLLFHFRIK-RRRRRRRR-NH<sub>2</sub>  
 17 Ac-EEIIRKLLQQLLFHFRIK-RRRRRRRR-NH<sub>2</sub>

**Figure 3.** Amino acid sequences of compounds 11–17, into which Glu-Lys pairs have been introduced.

**Table 2**

IC<sub>50</sub> values of compounds 5 and 11–17 toward the 3'-end processing and strand transfer reactions catalyzed by HIV-1 IN

Compound	IC <sub>50</sub> (μM)	
	3'-End processing	Strand transfer
5	0.09 ± 0.01	0.04 ± 0.01
11	0.05 ± 0.01	0.01 ± 0.001
12	0.12 ± 0.01	0.047 ± 0.01
13	0.14 ± 0.02	0.065 ± 0.01
14	0.23 ± 0.03	0.15 ± 0.002
15	0.04 ± 0.01	0.031 ± 0.01
16	0.71 ± 0.21	0.06 ± 0.004
17	0.18 ± 0.06	0.08 ± 0.02

strand transfer reaction (compound 16), indicating that Leu<sup>11</sup> and/or Phe<sup>15</sup> are indispensable for activity, especially for inhibition against 3'-end processing. Compound 17 has two substitutions of Glu-Lys for His<sup>14</sup>-Gly<sup>18</sup> and for Ala<sup>2</sup>-Ile<sup>6</sup>, which are common to compounds 11 and 12, respectively. A twofold decrease in both IN inhibitory activities of compound 17 is mostly due to the substitution for Ala<sup>2</sup>-Ile<sup>6</sup> common to 12, although 17 is slightly less active than 12 in both IN inhibitory assays.

Anti-HIV activity of these compounds was assessed by an MT-4 Luc system, in which MT-4 cells were stably transduced with the firefly luciferase expression cassette by a murine leukemia viral vector. MT-4 Luc cells constitutively express high levels of luciferase. HIV-1 infection significantly reduces luciferase expression due to the high susceptibility of MT-4 cells to HIV-1 infection. Protection of MT-4 Luc cells from HIV-1-induced cell death maintains the luciferase signals at high levels. In addition, the cytotoxicity of test compounds can be evaluated by a decrease of luciferase signals in these MT-4 Luc systems. The parent compound 5 showed significant anti-HIV activity at concentrations above 1.25 μM, as reported previously (Fig. 4).<sup>4</sup> Compound 15 showed a significant inhibitory effect against HIV-1 replication, and is thus comparable to compound 5. Compounds 11, 14 and 16 also displayed weak antiviral effects at concentrations of 2.5 and 5.0 μM and compounds 12, 13 and 17 failed to show any significant anti-HIV activity. These results suggest that there is a positive correlation between IN inhibitory activity and anti-HIV activity of the compounds. None of these compounds showed significant cytotoxic effects at concentrations below 5.0 μM.

The structures of compounds 5 and 11–17 were assessed by CD spectroscopy. Because the aqueous solubility of these peptides is not high the peptides were dissolved in 0.1 M phosphate buffer, containing 50% MeOH at pH 5.6. The CD spectra suggest that the parent compound 5, which has no Glu-Lys pair, forms a typical α-helical structure, and the other compounds, with the exception of 11 and 15, form α-helical structures similarly (Fig. 5). The order of strength of α-helicity is 12, 16 > 14 > 17 > 5 > 13. Compounds 11 and 15 have no characteristic pattern, although IN inhibitory activities of both compounds are superior to that of the parent



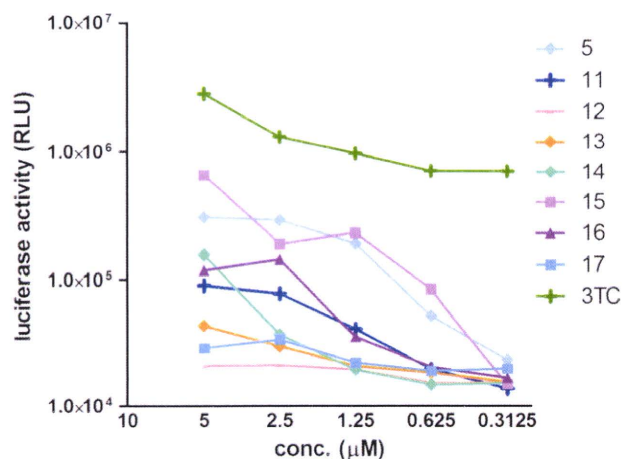


**Figure 4.** Luciferase signals in MT-4 Luc cells infected with HIV-1 in the presence of different concentrations of compounds **11–17**. Luciferase activity is expressed as relative luciferase units (RLU). 3TC is an HIV reverse transcriptase inhibitor, which was used as a positive control.

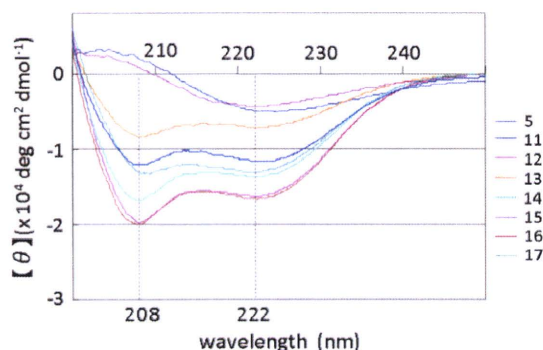


**Figure 5.** CD spectra of compounds **5** and **11–17** (5 μM) in 0.1 M phosphate buffer, pH 5.6 containing 50% MeOH at 25 °C.

compound **5**. Replacement of His<sup>14</sup>-Gly<sup>18</sup> and Ile<sup>3</sup>-Leu<sup>7</sup> by Glu-Lys in compounds **11** and **15**, respectively, caused a significant decrease in  $\alpha$ -helicity, possibly due to formation of unfavorable salt bridges such as Glu<sup>14</sup>-Arg<sup>16</sup> and Glu<sup>3</sup>-Arg<sup>5</sup>. Introduction of a Glu-Lys pair into Gln<sup>9</sup>-Ile<sup>13</sup> in compound **13** caused a slight decrease in  $\alpha$ -helicity, possibly due to interference in the formation of a salt bridge of Glu<sup>1</sup>-Arg<sup>5</sup> by that of Arg<sup>5</sup>-Glu<sup>9</sup>. In the other analogs, increases in  $\alpha$ -helicity were observed to result from the introduction of Glu-Lys pairs as we had initially postulated. Overall, there is no positive correlation between IN inhibitory or anti-HIV activity and the degree of  $\alpha$ -helicity of the compounds.

In order to identify the amino acid residues responsible for IN inhibitory and anti-HIV activities of these peptides, an Ala-scan of compound **4** was performed (Fig. 6). Compounds **18–22**, **25**, **27** and **29** showed IN inhibitory activities against the 3'-end processing and strand transfer reactions similar to those of **4** (Table 3). Ala-substitution for Leu<sup>7</sup>, Gln<sup>8</sup>, Gln<sup>9</sup>, Leu<sup>10</sup>, Leu<sup>11</sup>, His<sup>14</sup>, Arg<sup>16</sup> or Gly<sup>18</sup> did not cause any significant change in either of IN inhibitory activities, indicating that the replaced amino acids are not essential for IN inhibition. Ala-substitution for Phe<sup>12</sup>, Ile<sup>13</sup>, Phe<sup>15</sup> or Ile<sup>17</sup> gave compounds **23**, **24**, **26** and **28**, which were 2–4 times less active in both the IN inhibitory assays, suggesting that Phe<sup>12</sup>, Ile<sup>13</sup>, Phe<sup>15</sup> and Ile<sup>17</sup> are indispensable for IN inhibition. Assessment of anti-HIV activity in the MT-4 Luc system showed that all compounds **18–29** produced dose-dependent inhibition of HIV-1 replication, although they displayed cytotoxicity at 10 μM (**4**, **19–23**, **26** and **27**) or above 5 μM (**24** and **25**) (Fig. 7). Compounds **23** and **24**,

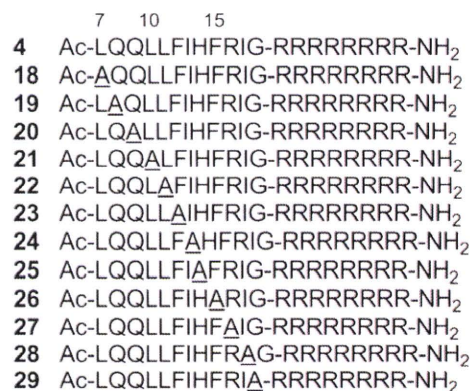


**Figure 6.** Amino acid sequences of compounds **18–29** based on an Ala-scan of compound **4**. Position numbers correspond to alignment with compound **5**.

**Table 3**

IC<sub>50</sub> values of compounds **18–29** toward the 3'-end processing and strand transfer reactions catalyzed by HIV-1 IN

Compound	IC <sub>50</sub> (μM)	
	3'-End processing	Strand transfer
<b>4</b>	0.11 ± 0.03	0.05 ± 0.01
<b>18</b>	0.12 ± 0.004	0.08 ± 0.01
<b>19</b>	0.13 ± 0.02	0.06 ± 0.01
<b>20</b>	0.10 ± 0.004	0.06 ± 0.01
<b>21</b>	0.12 ± 0.02	0.07 ± 0.01
<b>22</b>	0.13 ± 0.003	0.06 ± 0.01
<b>23</b>	0.34 ± 0.06	0.18 ± 0.03
<b>24</b>	0.33 ± 0.02	0.22 ± 0.01
<b>25</b>	0.13 ± 0.01	0.06 ± 0.01
<b>26</b>	0.25 ± 0.02	0.12 ± 0.01
<b>27</b>	0.11 ± 0.01	0.05 ± 0.01
<b>28</b>	0.20 ± 0.03	0.16 ± 0.02
<b>29</b>	0.09 ± 0.01	0.09 ± 0.01

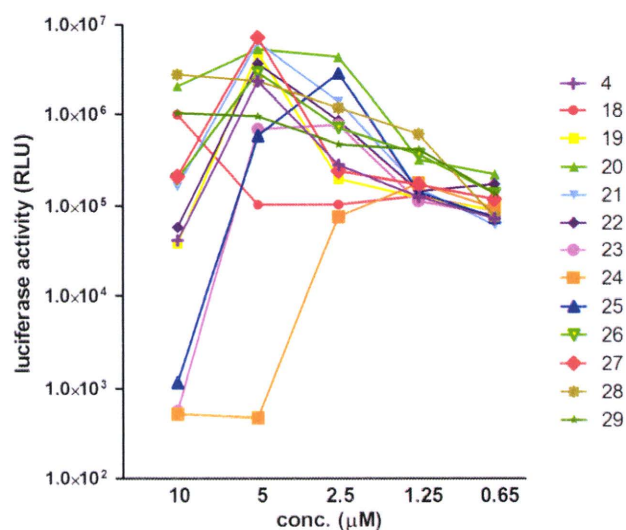


**Figure 7.** Luciferase signals in MT-4 Luc cells infected with HIV-1 in the presence of various concentrations of compounds **18–29**. Luciferase activity was valued as RLU.

with Ala-substitution for Phe<sup>12</sup> and Ile<sup>13</sup>, respectively, showed weaker inhibitory activity than **4** at 5 μM. Consequently, Phe<sup>12</sup> and Ile<sup>13</sup> were deemed to be critical for activity, which is consistent with the IN inhibitory activity results. A control peptide isomer of **5** (Ac-QIFEHLAGIIQLRFLRI-R<sub>8</sub>-NH<sub>2</sub>) did not show anti-HIV activity at



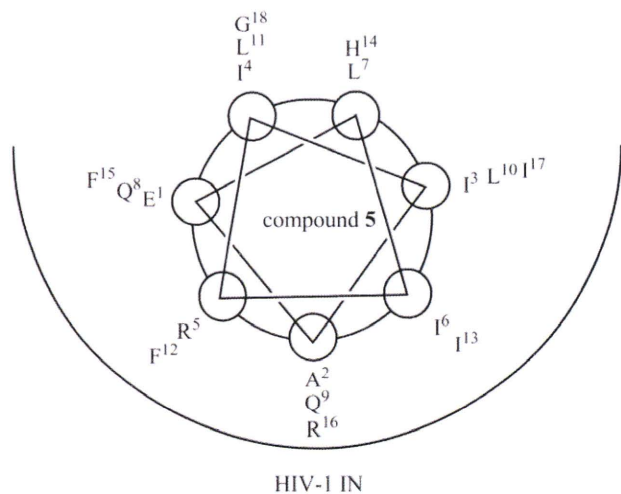


**Figure 8.** Brief presumed drawing of the binding model of HIV-1 IN and compound 5.

concentrations below 10  $\mu\text{M}$ , suggesting that the original Vpr-sequence, with the exceptions of Phe<sup>12</sup>, Ile<sup>13</sup>, Phe<sup>15</sup> and Ile<sup>17</sup>, is critical for activity.

The assumption that compound **5** forms an  $\alpha$ -helical structure when binding to HIV-1 IN suggests the binding model of IN and **5** shown in Figure 8, as **5** forms an  $\alpha$ -helical structure in 50% aqueous MeOH solution. In this model, Phe<sup>12</sup>, Ile<sup>13</sup>, Phe<sup>15</sup> and Ile<sup>17</sup>, which were identified by the Ala-scan experiment as critical residues, are located in the pocket of IN. His<sup>14</sup> and Gly<sup>18</sup>, which can be replaced by Glu-Lys with an increase of activity in compound **11**, are located outside of the pocket of IN. Ile<sup>3</sup> and Leu<sup>7</sup> can also be replaced by Glu-Lys while retaining activity in compound **15**, and Leu<sup>7</sup> is located outside of the pocket, whereas Ile<sup>3</sup> is located in the edge of the pocket. Compounds **11** and **15** might form  $\alpha$ -helical structures when binding to IN, although **11** or **15** does not show  $\alpha$ -helicity in the CD spectrum. Thus, these compounds might retain IN inhibitory activity. This binding model is compatible with the results of structure–activity relationship studies involving Glu-Lys substitution and Ala-scan. The reason for decreases in IN inhibitory and anti-HIV activity of compounds **12** and **17**, which show increases of  $\alpha$ -helicity, are possibly due to substitution of Glu-Lys for Ala<sup>2</sup> and Ile<sup>6</sup>, which are located in the pocket of IN. The reason for a decrease in activity of compounds **14** and **16**, which show increased  $\alpha$ -helicity, might be due to substitution of Lys for Gln<sup>8</sup> and Phe<sup>15</sup>, respectively, which are located in the pocket of IN. The reason for decreases in IN inhibitory and anti-HIV activity of compound **13**, which also shows a decrease of  $\alpha$ -helicity, are possibly due to substitution of Glu-Lys for Gln<sup>9</sup> and Ile<sup>13</sup>, which are located in the pocket of IN.

### 3. Conclusion

In the present study, structure–activity relationship studies were performed on Vpr-derived peptides **4** and **5**, which had been previously identified as HIV-1 IN inhibitors.<sup>4</sup> The Glu-Lys substitution experiments and Ala-scan data suggest that several amino acid residues of **4** and **5** are indispensable for IN inhibitory and anti-HIV activities, and a binding model of IN and **5** were proposed. Furthermore, two novel compounds **11** and **15**, which contained Glu-Lys pairs and showed more potent IN inhibitory activities than compound **5**, were found. These data including the binding model should be useful for the development of potent HIV-1 IN inhibitors based on Vpr-peptides.

## 4. Experimental

### 4.1. Chemistry

All peptides were synthesized by the Fmoc-based solid-phase method. The synthetic peptides were purified by RP-HPLC and identified by ESI-TOF-MS. Fmoc-protected amino acids and reagents for peptide synthesis were purchased from Novabiochem, Kokusan Chemical Co., Ltd and Watanabe Chemical Industries, Ltd. Protected peptide resins were constructed on NovaSyn TGR resins (0.26 meq/g, 0.025 and 0.0125 mmol scales for Glu-Lys substitution and Ala-scan peptides, respectively). All peptides were synthesized by stepwise elongation techniques. Each cycle involves (i) deprotection of an Fmoc group with 20% (v/v) piperidine/DMF (10 mL) for 15 min and (ii) coupling with 5.0 equiv of Fmoc-protected amino acid, 5.0 equiv of diisopropylcarbodiimide (DIPCI) and 5.0 equiv of 1-hydroxybenzotriazole monohydrate (HOBt·H<sub>2</sub>O) in DMF (3 mL) for 90 min. N-Terminal  $\alpha$ -amino groups of Glu-Lys substitution and Ala-scan peptides were acetylated with 100 equiv of acetic anhydride in DMF (10 mL). Cleavage from the resin and side chain deprotection were carried out by stirring for 1.5 h with *m*-cresol (0.25 mL), thioanisole (0.75 mL), 1,2-ethanedithiol (0.75 mL) and TFA (8.25 mL). After removal of the resins by filtration, the filtrate was concentrated under reduced pressure, the crude peptides were precipitated in cooled diethyl ether and purified by preparative RP-HPLC on a Cosmosil 5C18-AR II column (10  $\times$  250 mm, Nacalai Tesque, Inc.) with a LaChrom Elite HTA system (Hitachi). The HPLC solvents employed were water containing 0.1% TFA (solvent A) and acetonitrile containing 0.1% TFA (solvent B). All peptides were purified using a linear gradient of solvents A and B over 30 min at a flow rate of 3 cm<sup>3</sup> min<sup>-1</sup>. The purified peptides were identified by ESI-TOF-MS (Bruker Daltonics micrOTOF-2focus) (shown in Table S1 in Supplementary data). All peptides were obtained after lyophilization as fluffy white powders of the TFA salts. The purities of these peptides were checked by analytical HPLC on a Cosmosil 5C18-ARII column (4.6  $\times$  250 mm, Nacalai Tesque, Inc.) eluted with a linear gradient of solvents A and B at a flow rate of 1 cm<sup>3</sup> min<sup>-1</sup>, and eluted products were detected by UV at 220 nm (shown in Figs. S1–S3 in Supplementary data).

### 4.2. Expression and purification of F185K/C280S HIV-1 integrase from *Escherichia coli*

Plasmid encoding IN1–288/F185K/C280S was expressed in *Escherichia coli* strain C41. The solubility of the mutant protein was examined in a crude cell lysate, as follows. Cells were grown in 1 L of culture medium containing 100  $\mu\text{g}/\text{mL}$  of ampicillin at 37  $^{\circ}\text{C}$  until the optical density of the culture at 600 nm was between 0.4 and 0.9. Protein expression was induced by the addition of isopropyl-1-thio- $\beta$ -D-galactopyranoside to a final concentration of 0.1 mM. After 2 h, the cells were collected by centrifugation at 6000 rpm for 30 min. After removal of the supernatant, the cells were resuspended in HED buffer (20 mM HEPES, pH 7.5, 1 mM EDTA, 1 mM DTT) with 0.5 mg/mL lysozyme and stored on ice for 30 min. The cells were sonicated until the solution exhibited minimal viscosity then it was centrifuged at 15,000 rpm for 30 min. After removal of the supernatant, the pellet was dissolved in TNM buffer (20 mM Tris/HCl, pH 8.0, 1 M NaCl, 2 mM 2-mercaptoethanol) with 5 mM imidazole and stored on ice for 30 min. The cells were then centrifuged at 15,000 rpm for 30 min and the supernatant was collected. The supernatant was then filtered through 0.45  $\mu\text{m}$  filter cartridge and applied to a HisTrap column at 1 mL/min flow rate. After loading, the column was washed with 10 volume of TNM buffer with 5 mM imidazole. Protein was eluted with a linear gradient of 500 mM imidazole, containing TNM buf-



fer. Fractions containing IN were pooled and checked with SDS-PAGE.

#### 4.3. CD spectroscopy of peptides with Glu-Lys substitution

CD measurements were performed on a JASCO J720 spectropolarimeter equipped with thermo-regulator (JASCO Corp., Ltd), using 5  $\mu$ M of peptides dissolved in 0.1 M phosphate buffer, pH 5.6 containing 50% MeOH. UV spectra were recorded at 25 °C in a quartz cell 1.0 mm path length, a time constant of 1 s, and a 100 nm/min scanning speed with 0.1 nm resolution.

#### 4.4. Integrase assays

Expression and purification of the recombinant IN in *E. coli* were performed as previously reported with addition of 10% glycerol to all buffers. Oligonucleotide substrates were prepared as described.<sup>6</sup> Integrase reactions were performed in 10  $\mu$ L with 400 nM of recombinant IN, 20 nM of 5'-end [<sup>32</sup>P]-labeled oligonucleotide substrate and inhibitors at various concentrations. Solutions of 10% DMSO without inhibitors were used as controls. Reaction mixtures were incubated at 37 °C (60 min) in buffer containing 50 mM MOPS, pH 7.2, 7.5 mM MgCl<sub>2</sub>, and 14.3 mM 2-mercaptoethanol. Reactions were stopped by addition of 10  $\mu$ L of loading dye (10 mM EDTA, 98% deionized formamide, 0.025% xylene cyanol and 0.025% bromophenol blue). Reactions were then subjected to electrophoresis in 20% polyacrylamide–7 M urea gels. Gels were dried and reaction products were visualized and quantitated with a Typhoon 8600 (GE Healthcare, Little Chalfont, Buckinghamshire, UK). Densitometric analyses were performed using ImageQuant from Molecular Dynamics Inc. The concentrations at which enzyme activity was reduced by 50% (IC<sub>50</sub>) were determined using 'Prism' software (GraphPad Software, San Diego, CA) for nonlinear regression to fit dose–response data to logistic curve models.

#### 4.5. Replication assays (MT-4 luciferase assays)

MT-4 luciferase cells ( $1 \times 10^3$  cells) grown in 96-well plates were infected with HIV-1<sub>HXB2</sub> in the presence of various concentrations of peptides. At 6–7 days post-infection, cells were lysed and the luciferase activities were measured using the Steady-Glo assay kit (Promega), according to the manufacturer's protocol. Chemiluminescence was detected with a Veritas luminometer (Promega).

#### Acknowledgments

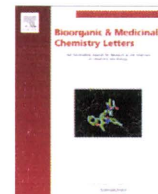
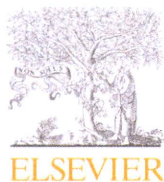
N.O. and T.T. are supported by JSPS research fellowships for young scientists. This work was supported by Mitsui Life Social Welfare Foundation, Grant-in-Aid for Scientific Research from the Ministry of Education, Culture, Sports, Science, and Technology of Japan, the Health and Labour Sciences Research Grants from Japanese Ministry of Health, Labor, and Welfare, and by the NIH Intramural Program, Center for Cancer Research, US National Cancer Institute.

#### Supplementary data

Supplementary data associated with this article can be found, in the online version, at doi:10.1016/j.bmc.2010.07.050.

#### References and notes

- Mitsuya, H.; Erickson, J. In *Textbook of AIDS Medicine*; Merigan, T. C., Bartlett, J. G., Bolognesi, D., Eds.; Williams & Wilkins: Baltimore, 1999; pp 751–780.
- (a) Cahn, P.; Sued, O. *Lancet* **2007**, 369, 1235; (b) Grinsztejn, B.; Nguyen, B.-Y.; Katlama, C.; Gatell, J. M.; Lazzarin, A.; Vittecoq, D.; Gonzalez, C. J.; Chen, J.; Harvey, C. M.; Isaacs, R. D. *Lancet* **2007**, 369, 1261.
- (a) Farnet, C. M.; Bushman, F. D. *Cell* **1997**, 88, 483; (b) Chen, H.; Engelman, A. *Proc. Natl. Acad. Sci. U.S.A.* **1998**, 95, 15270; (c) Gleenberg, I. O.; Herschhorn, A.; Hizi, A. *J. Mol. Biol.* **2007**, 369, 1230; (d) Gleenberg, I. O.; Avidan, O.; Goldgur, Y.; Herschhorn, A.; Hizi, A. *J. Biol. Chem.* **2005**, 280, 21987; (e) Hehl, E. A.; Joshi, P.; Kalpana, G. V.; Prasad, V. R. *J. Virol.* **2004**, 78, 5056; (f) Tasara, T.; Maga, G.; Hottiger, M. O.; Hubscher, U. *FEBS Lett.* **2001**, 507, 39; (g) Gleenberg, I. O.; Herschhorn, A.; Goldgur, Y.; Hizi, A. *Arch. Biochem. Biophys.* **2007**, 458, 202.
- Suzuki, S.; Urano, E.; Hashimoto, C.; Tsutsumi, H.; Nakahara, T.; Tanaka, T.; Nakanishi, Y.; Maddali, K.; Han, Y.; Hamatake, M.; Miyauchi, K.; Pommier, Y.; Beutler, J. A.; Sugiura, W.; Fuji, H.; Hoshino, T.; Itotani, K.; Nomura, W.; Narumi, T.; Yamamoto, N.; Komano, J. A.; Tamamura, H. *J. Med. Chem.* **2010**, 53, 5356.
- Suzuki, T.; Futaki, S.; Niwa, M.; Tanaka, S.; Ueda, K.; Sugiura, Y. *J. Biol. Chem.* **2002**, 277, 2437.
- (a) Yan, H.; Mizutani, T. C.; Nomura, N.; Tanaka, T.; Kitamura, Y.; Miura, H.; Nishizawa, M.; Tatsumi, M.; Yamamoto, N.; Sugiura, W. *Antivir. Chem. Chemother.* **2005**, 16, 363; (b) Marchand, C.; Zhang, X.; Pais, G. C. G.; Cowansage, K.; Neamati, N.; Burke, T. R., Jr.; Pommier, Y. *J. Biol. Chem.* **2002**, 277, 12596; (c) Semenova, E. A.; Johnson, A. A.; Marchand, C.; Davis, D. A.; Tarchoan, R.; Pommier, Y. *Mol. Pharmacol.* **2006**, 69, 1454; (d) Leh, H.; Brodin, P.; Bischerour, J.; Deprez, E.; Tauc, P.; Brochon, J. C.; LeCam, E.; Coulaud, D.; Auclair, C.; Mouscadet, J. F. *Biochemistry* **2000**, 39, 9285; (e) Marchand, C.; Neamati, N.; Pommier, Y. In *In Vitro Human Immunodeficiency Virus Type 1 Integrase Assays. In Methods in Enzymology (Drug-Nucleic Acid Interactions)*; Chaires, J. B., Waring, M. J., Eds.; Elsevier: Amsterdam, 2001; Vol. 340, pp 624–633.
- Morellet, N.; Bouaziz, S.; Petitjean, P.; Roques, B. P. *J. Mol. Biol.* **2003**, 327, 215.



## CD4 mimics targeting the HIV entry mechanism and their hybrid molecules with a CXCR4 antagonist

Tetsuo Narumi<sup>a</sup>, Chihiro Ochiai<sup>a</sup>, Kazuhisa Yoshimura<sup>b</sup>, Shigeyoshi Harada<sup>b</sup>, Tomohiro Tanaka<sup>a</sup>, Wataru Nomura<sup>a</sup>, Hiroshi Arai<sup>a</sup>, Taro Ozaki<sup>a</sup>, Nami Ohashi<sup>a</sup>, Shuzo Matsushita<sup>b</sup>, Hirokazu Tamamura<sup>a,\*</sup>

<sup>a</sup>Institute of Biomaterials and Bioengineering, Tokyo Medical and Dental University, Chiyoda-ku, Tokyo 101-0062, Japan

<sup>b</sup>Center for AIDS Research, Kumamoto University, Kumamoto 860-0811, Japan

### ARTICLE INFO

#### Article history:

Received 14 June 2010

Revised 22 July 2010

Accepted 26 July 2010

Available online 3 August 2010

#### Keywords:

CD4

HIV entry

Hybrid molecule

gp120

### ABSTRACT

Small molecules behaving as CD4 mimics were previously reported as HIV-1 entry inhibitors that block the gp120–CD4 interaction and induce a conformational change in gp120, exposing its co-receptor-binding site. A structure–activity relationship (SAR) study of a series of CD4 mimic analogs was conducted to investigate the contribution from the piperidine moiety of CD4 mimic **1** to anti-HIV activity, cytotoxicity, and CD4 mimicry effects on conformational changes of gp120. In addition, several hybrid molecules based on conjugation of a CD4 mimic analog with a selective CXCR4 antagonist were also synthesized and their utility evaluated.

© 2010 Elsevier Ltd. All rights reserved.

The infection of host cells by HIV-1 takes place in multiple steps via a dynamic supramolecular mechanism mediated by two viral envelope glycoproteins (gp41, gp120) and several cell surface proteins (CD4, CCR5/CXCR4).<sup>1</sup> Cell penetration begins with the interaction of gp120 with the primary receptor CD4. This induces conformational changes in gp120, leading to the exposure of its V3 loop allowing the subsequent binding of gp120 to a co-receptor, CCR5<sup>2</sup> or CXCR4.<sup>3</sup>

*N*-(4-Chlorophenyl)-*N'*-(2,2,6,6-tetramethyl-piperidin-4-yl)oxalamide (NBD-556: **1**) and the related compounds NBD-557 (**2**) and YYA-021 (**3**) have been identified as a novel class of HIV-1 entry inhibitors, which exert potent cell fusion and virus cell fusion inhibitory activity at low micromolar levels (Fig. 1).<sup>4</sup> Furthermore, compound **1** can also induce thermodynamically favored conformational changes in gp120 similar to those caused by CD4 binding. The X-ray crystal structure of gp120 complexed with CD4 revealed the presence of a hydrophobic cavity, the Phe43 cavity, which is penetrated by the aromatic ring of Phe<sup>43</sup> of CD4.<sup>5</sup> Molecular modeling revealed that compound **1** is also inserted into the Phe43 cavity, the *para*-chlorophenyl group of **1** entering more deeply than the phenyl ring of Phe<sup>43</sup> of CD4 and interacting with the conserved gp120 residues such as Trp<sup>427</sup>, Phe<sup>382</sup>, and Trp<sup>112</sup>.<sup>4c</sup> The modeling also suggested that an oxalamide linker forms hydrogen bonds with carbonyl groups of the gp120 backbone peptide bonds. Our model of **1** docked into gp120 revealed that eight other gp120

residues, Val<sup>255</sup>, Asp<sup>368</sup>, Glu<sup>370</sup>, Ser<sup>375</sup>, Ile<sup>424</sup>, Trp<sup>427</sup>, Val<sup>430</sup>, and Val<sup>475</sup> are located within a 4.4 Å-radius of **1** and that a large cavity exists around the *p*-position of the aromatic ring of **1**.<sup>4e</sup> Based on these observations, we conducted a structure–activity relationship (SAR) study of a series of analogs of CD4 mimics with substituents at the *p*-position of the aromatic ring. This study revealed that a certain size and electron-withdrawing ability of the substituents are indispensable for potent anti-HIV activity.<sup>4e</sup>

Although several reported SAR studies of **1** have revealed the contributions of the phenyl ring and the oxalamide linker of **1** to the binding affinity with gp120, the anti-HIV activity and the CD4 mimicry on conformational changes of gp120,<sup>4</sup> there has been, to the best of our knowledge, no prior report describing SAR studies of the piperidine ring of **1**. In this paper, the contributions of the piperidine ring of **1** to the anti-HIV activity, CD4 mimicry and cytotoxicity were investigated through the SAR studies focused on the piperidine ring of **1**. Furthermore, to apply the utility of CD4 mimics to the development of potent anti-HIV agents, a series of the

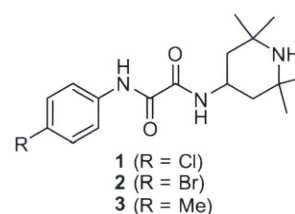


Figure 1. NBD-556 (**1**) and related compounds.

\* Corresponding author.

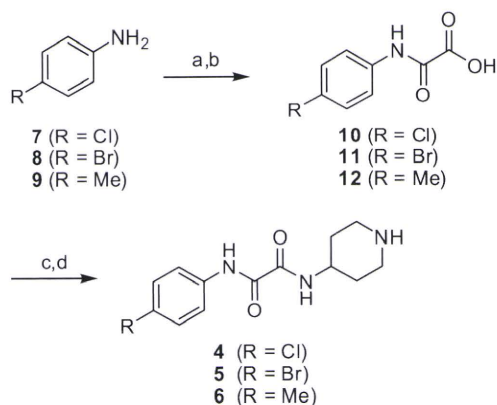
E-mail address: [tamamura.mr@tmd.ac.jp](mailto:tamura.mr@tmd.ac.jp) (H. Tamamura).



hybrid molecules that combined CD4 mimic analogs with a selective CXCR4 antagonist were also synthesized and bioevaluated.

For the design of novel CD4 mimic analogs, we initially tried to directly derivatize the nitrogen atom of piperidine group. However, direct alkylation and acylation of **1** failed probably as a result of steric hindrance from the methyl groups on the piperidine ring so we synthesized several derivatives lacking the methyl groups and evaluated their anti-HIV activity, cytotoxicity, and ability to mimic CD4. According to the previous SAR study,<sup>4e</sup> the *p*-Cl (**4**), *p*-Br (**5**) and *p*-methyl derivatives (**6**) lacking the methyl groups on the piperidine ring were prepared. Compounds **4–6** were synthesized by published methods as shown in Scheme 1. Briefly, coupling of aniline derivatives with ethyl chloroglyoxalate in the presence of Et<sub>3</sub>N and subsequent saponification gave the corresponding acids (**10–12**). Condensation of these acids with 4-amino-*N*-benzylpiperidine in the presence of EDC-HOBt system, followed by debenzylation under von Braun conditions with 1-chloroethyl chloroformate<sup>6</sup> produced the desired compounds **4–6**.<sup>7</sup>

The anti-HIV activity of each of the synthetic compounds was evaluated against MNA (R5) strain, with the results shown in Table 1. IC<sub>50</sub> values were determined by the 3-(4,5-dimethylthiazol-2-yl)-2,5-diphenyltetrazolium bromide (MTT) method<sup>8</sup> as the concentrations of the compounds which conferred 50% protection against HIV-1-induced cytopathogenicity in PM1/CCR5 cells. Cytotoxicity of the compounds based on the viability of mock-infected PM1/CCR5 cells was also evaluated using the MTT method. CC<sub>50</sub> values, the concentrations achieving 50% reduction of the viability of mock-infected cells, were also determined. Compounds **1** and **3** showed potent anti-HIV activity. The anti-HIV IC<sub>50</sub> of compound **2** was previously reported to be comparable to that of compound **1**,



**Scheme 1.** Synthesis of compounds **4–6**. Reagents and conditions: (a) ethyl chloroglyoxalate, Et<sub>3</sub>N, THF; (b) 1 M aq NaOH, THF, 67%–quant.; (c) 1-benzyl-4-aminopiperidine, EDC-HCl, HOBt-H<sub>2</sub>O, Et<sub>3</sub>N, THF; (d) (i) 1-chloroethyl chloroformate, CH<sub>2</sub>Cl<sub>2</sub>; (ii) MeOH, 8–47%.

**Table 1**  
Effects of the methyl groups on anti-HIV activity and cytotoxicity of CD4 mimic analogs<sup>a</sup>

Compd	R	IC <sub>50</sub> (μM) MNA (R5)	CC <sub>50</sub> (μM)
<b>1</b>	Cl	12	110
<b>2</b>	Br	ND	93
<b>3</b>	Me	15	210
<b>4</b>	Cl	8	100
<b>5</b>	Br	6	50
<b>6</b>	Me	20	190

<sup>a</sup> All data with standard deviation are the mean values for at least three independent experiments (ND = not determined).

and thus was not determined in this study. Novel derivatives **4** and **6** without the methyl groups on the piperidine ring, showed significant anti-HIV activity comparable to that of the parent compounds **1** and **3**, respectively. The *p*-methyl derivative **6** has slightly lower activity than the *p*-Cl derivative **4** and the *p*-Br derivative **5**. These results are consistent with our previous SAR studies on the parent compounds **1–3**. Compound **5** was found to exhibit relatively strong cytotoxicity (CC<sub>50</sub> = 50 μM) and compounds **4** and **6** have cytotoxicities comparable to that of compounds **1** and **3**, respectively. This observation indicates that the methyl groups on the piperidine ring do not contribute significantly to the anti-HIV activity or the cytotoxicity.

Compound **1** and the newly synthesized derivatives **4–6** were also evaluated for their effects on conformational changes of gp120 by a fluorescence activated cell sorting (FACS) analysis. The profile of binding of an anti-envelope CD4-induced monoclonal antibody (4C11) to the Env-expressing cell surface (an R5-HIV-1 strain, JR-FL, -infected PM1 cells) pretreated with the above derivatives was examined. Comparison of the binding of 4C11 to the cell surface was measured in terms of the mean fluorescence intensity (MFI), as shown in Figure 2. Pretreatment of the Env-expressing cell surface with compound **1** (MFI = 53.66) produced a significant increase in binding affinity for 4C11, consistent with that reported previously.<sup>4e</sup> This indicates that compound **1** enhances the binding affinity of gp120 with the 17b monoclonal antibody which recognizes CD4-induced epitopes on gp120. The Env-expressing cells without CD4 mimic-pretreatment failed to show significant binding affinity to 4C11. On the other hand, the profiles of the binding of 4C11 to the Env-expressing cell surface pretreated with compound **4** (Cl derivative) and **5** (Br derivative) (MFI = 49.88 and 52.34) were similar to that of compound **1**. Pretreatment of the cell surface with compound **6** (Me derivative) (MFI = 45.99) produced slightly lower enhancement but significant levels of binding affinity for 4C11, compared to that of compound **1** as pretreatments. These results suggested that the removal of the methyl groups on the piperidine moiety might not affect the CD4 mimicry effects on conformational changes of gp120 and it was conjectured that the phenyl ring of CD4 mimic might be a key moiety for the interaction with gp120 to induce the conformational changes of gp120. This is consistent with the results in the previous paper where it was reported that CD4 mimics having suitable substituent(s) on the phenyl ring cause a conformational change, resulting in external exposure of the co-receptor-binding site of gp120.<sup>4e</sup>

Based on these results, a series of *N*-alkylated and *N*-acylated piperidine derivatives **13–18** with no methyl groups were prepared. Several compounds with 6-membered rings were also prepared to determine whether or not the piperidine ring is mandatory. The synthesis of these derivatives is shown in Scheme 2. Since the *p*-Cl derivative **4** showed potent anti-HIV activity and relatively low cytotoxicity, compared to the *p*-Br derivative **5**, chlorine was selected as the substituent at the *p*-position of the phenyl ring. The *N*-methyl derivative **13** was synthesized by coupling of **10** with 4-amine-1-methylpiperidine. Alkylation of **4** with *tert*-butyl bromoacetate, followed by deprotection of *tert*-butyl ester provided compound **14**. The *N*-isopropyl derivative **15** was prepared by reductive amination of **4** with isopropyl aldehyde. The *N*-acyl derivatives **16–18** were prepared by simple acylation or condensation with the corresponding substrate. The synthesis of other derivatives **19–23** with different 6-membered rings is depicted in Scheme 3. The 6-membered ring derivatives with the exception of **21** were prepared by coupling of acid **10** with the corresponding amines. Compound **21** was prepared by reaction of **10** with thionyl chloride to give the corresponding acid chloride, which was subsequently coupled with 4-aminopyridine.

Compounds **1**, **3**, and **13–18** were evaluated for their CD4 mimicry effects on conformational changes of gp120 by the FACS anal-



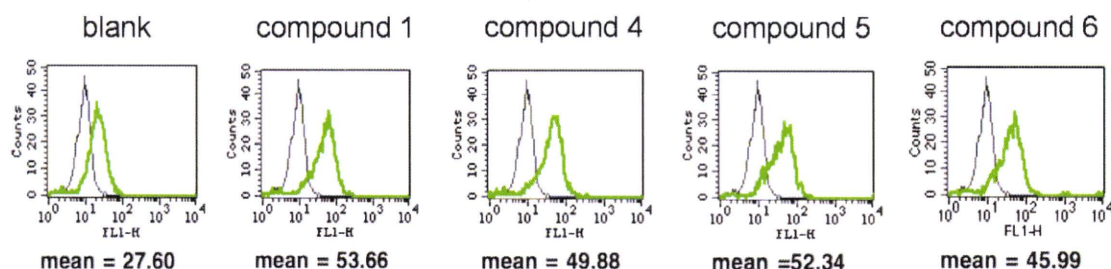
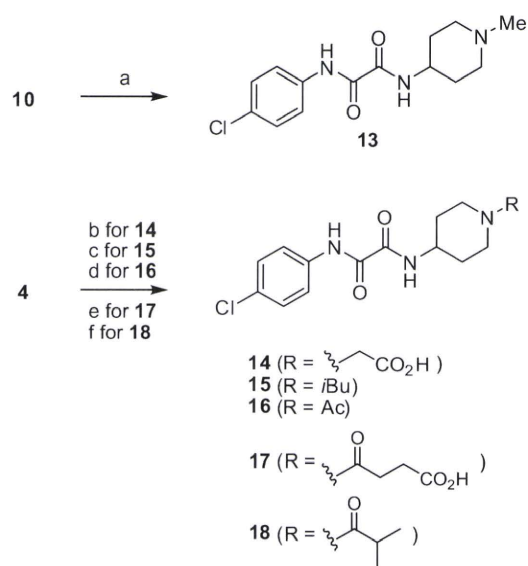
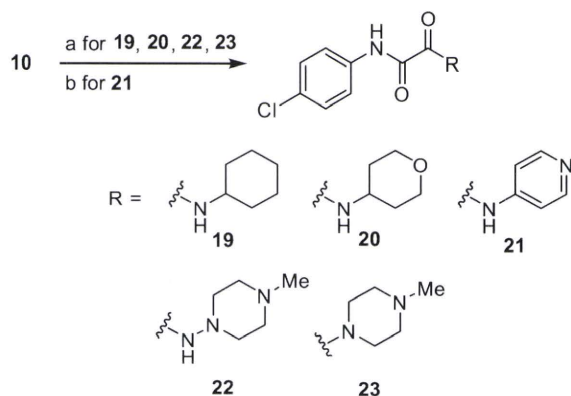


**Figure 2.** FACS analysis of compounds **1** and **4–6**. JR-FL (R5, Sub B) chronically infected PM1 cells were preincubated with 100  $\mu\text{M}$  of a CD4 mimic for 15 min, and then incubated with an anti-HIV-1 mAb, 4C11, at 4  $^{\circ}\text{C}$  for 15 min. The cells were washed with PBS, and fluorescein isothiocyanate (FITC)-conjugated goat anti-human IgG antibody was used for antibody-staining. Flow cytometry data for the binding of 4C11 (green lines) to the Env-expressing cell surface in the presence of a CD4 mimic are shown among gated PM1 cells along with a control antibody (anti-human CD19; black lines). Data are representative of the results from a minimum of two independent experiments. The number at the bottom of each graph shows the mean fluorescence intensity (MFI) of the antibody 4C11.



**Scheme 2.** Synthesis of N-alkylated and N-acylated piperidine derivatives **13–18**. Reagents and conditions: (a) 4-amine-1-methylpiperidine, EDC-HCl, HOBT-H<sub>2</sub>O, Et<sub>3</sub>N, THF, 16%; (b) (i) *tert*-butyl bromoacetate, NaH, DMF; (ii) TFA, 6%; (c) isobutylaldehyde, NaBH(OAc)<sub>3</sub>, AcOH, DCE, quant.; (d) acetyl chloride, Et<sub>3</sub>N, DMF, quant.; (e) succinic anhydride, Et<sub>3</sub>N, THF, 37%; (f) isobutyric acid, EDC-HCl, HOBT-H<sub>2</sub>O, Et<sub>3</sub>N, THF, 95%.



**Scheme 3.** Synthesis of 6-membered ring derivatives **19–23**. Reagents and conditions: (a) the corresponding amine, EDC-HCl, HOBT-H<sub>2</sub>O, Et<sub>3</sub>N, THF, 22%–quant.; (b) 4-aminopyridine, SOCl<sub>2</sub>, MeOH, 38%.

4C11, similar to that observed in the pretreatment with compound **1**. The profile of the binding of 4C11 to the cell surface pretreated with compounds **14** and **17** was similar to that of controls, suggesting that these derivatives offer no significant enhancement of binding affinity for 4C11 and that the carboxylic moiety in the terminal of piperidine ring is not suited to CD4 mimicry. It is hypothesized that the carboxylic moieties of compounds **14** and **17** might prevent the interaction of CD4 mimic with gp120 by their multiple contacts with side chain(s) of amino acid(s) around the Phe43 cavity, such as Asp<sup>368</sup> and Glu<sup>370</sup>. Replacement of the piperidine moiety with the different 6-membered rings resulted in a significant loss of binding affinity for 4C11 in the FACS analysis of compound **19–23** (MFI(**19**) = 11.44, MFI(**20**) = 12.84, MFI(**21**) = 12.47, in MFI(blank) = 11.34; MFI(**22**) = 26.67, MFI(**23**) = 20.21, in MFI(blank) = 26.79, data not shown), indicating a significant contribution from the piperidine ring which interacts with gp120 inducing conformational changes.

In view of their ability to induce conformational changes of gp120, the anti-HIV activity and cytotoxicity of the piperidine derivatives **13–18** were further evaluated, with the results shown in Table 2. The anti-HIV activity of the synthetic compounds was evaluated against various viral strains including both laboratory and primary isolates and IC<sub>50</sub> and CC<sub>50</sub> values were determined as those of compounds **4–6**. The *N*-methylpiperidine compound **13**, was not found to possess significant anti-HIV activity against a primary isolate, but was found to possess moderate anti-HIV activity against a laboratory isolate, a IIB strain (IC<sub>50</sub> = 67  $\mu\text{M}$ ). Anti-HIV activity was not observed however, even at concentrations of 100  $\mu\text{M}$  of **13** against an 89.6 strain. The potency was approximately eight-fold lower than that of the parent compound **1** (IC<sub>50</sub> = 8  $\mu\text{M}$ ), indicating a partial contribution of the hydrogen atom of the amino group of the piperidine ring to the bioactivity of CD4 mimic. Although compound **15**, with an *N*-isobutylpiperidine moiety, failed to show significant anti-HIV activity against laboratory isolates, relatively potent activity was observed against a primary isolate, an MTA strain (IC<sub>50</sub> = 28  $\mu\text{M}$ ). Compounds **16** and **18**, which are *N*-acylpiperidines, were tested against laboratory isolates and significant anti-HIV activity was not observed even at 100  $\mu\text{M}$ . Compounds **14** and **17**, with the carboxylic moieties, failed to show significant anti-HIV activity against laboratory isolates even at 100  $\mu\text{M}$ , which are compatible with the FACS analysis. These results suggest that the *N*-substituent on the piperidine ring of CD4 mimic analogs may contribute to a critical interaction required for binding to gp120. Compounds **19–23** showed no significant anti-HIV activity against a IIB strain even at 100  $\mu\text{M}$ , which are compatible with the FACS analysis (data not shown).

All but one of the compounds **13–18** have no significant cytotoxicity to PM1/CCR5 cells (CC<sub>50</sub>  $\geq$  260  $\mu\text{M}$ ); the exception is compound **18** (CC<sub>50</sub> = 45  $\mu\text{M}$ ). Compounds **13** and **15** show relatively potent anti-HIV activity without significant cytotoxicity.

ysis, and the results are shown in Figure 3. Pretreatment of the Env-expressing cells with the *N*-substituted compounds **13**, **15**, **16**, and **18** produced a notable increase in binding affinity to

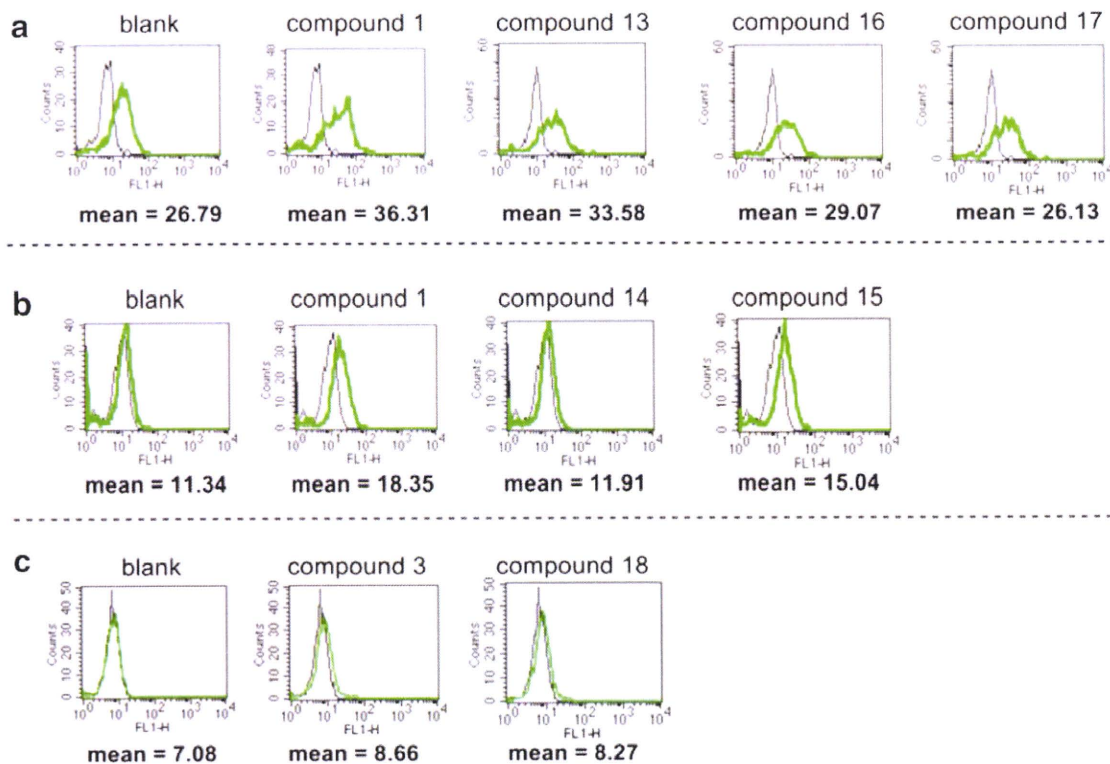


Figure 3. FACS analysis of compounds **1**, **3**, and **13–18**. The experimental procedures are described in Figure 2. The lanes of (a), (b) and (c) show independent experiments.

Table 2  
Anti-HIV activity and cytotoxicity of compounds **13–18**<sup>a</sup>

Compd	R	IC <sub>50</sub> (μM)			CC <sub>50</sub> (μM)
		Laboratory isolates		Primary isolates	
		IIIB (X4)	89.6 (dual)	MTA (R5)	
<b>1</b>	H	8	10	ND	150
<b>4</b>	H	ND	ND	ND	100
<b>13</b>	Me	67	>100	ND	>300
<b>14</b>	CH <sub>2</sub> CO <sub>2</sub> H	>100	ND	ND	260
<b>15</b>	iBu	>100	ND	28	>300
<b>16</b>	Ac	>100	>100	ND	>300
<b>17</b>	C(O)CH <sub>2</sub> CH <sub>2</sub> CO <sub>2</sub> H	>100	>100	ND	>300
<b>18</b>	C(O)iPr	>100	ND	ND	45

<sup>a</sup> All data with standard deviation are the mean values for at least three independent experiments.

The results for **15** showed it to have 3–6 times less cytotoxicity than **4** and **18**. This observation indicates that the alkylation of the piperidine nitrogen may be favorable because it lowers the cytotoxicity of CD4 mimic analogs.

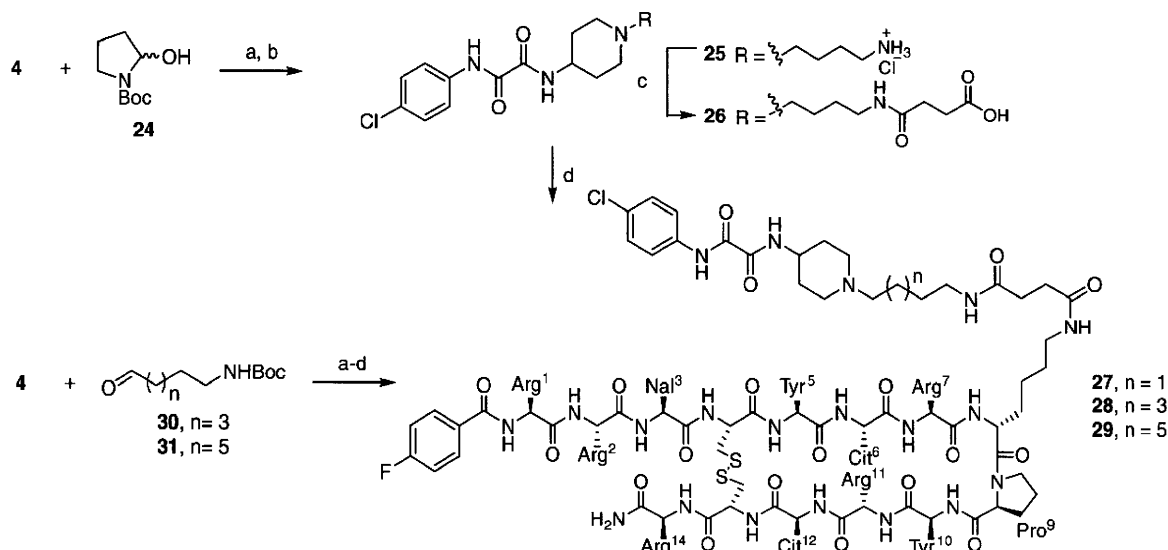
In the course of the SAR studies on CD4 mimic analogs, we have already found that a CD4 mimic or sCD4 exhibited a remarkable synergistic effect<sup>4e</sup> with a 14-mer peptide CXCR4 antagonist T140.<sup>9</sup> This result indicates that the interaction of CD4 mimic with gp120 could facilitate the approach of CXCR4 to gp120 by exposing the co-receptor binding site of gp120. It was thought that the CD4 mimic analogs conjugated with a selective CXCR4 antagonist might as a consequence show a higher synergistic effect for the improvement of anti-HIV activity. In this context, efforts were made to synthesize and bioevaluate hybrid molecules that combined a CD4 mimic analog with 4F-benzoyl-TZ14011, which is a derivative of T140 optimized for CXCR4 binding and stability in vivo.<sup>10</sup>

The synthesis of hybrid molecules **27–29** is outlined in Scheme 4. To examine the influence of the linker length on anti-HIV activity and cytotoxicity, three hybrid molecules with linkers of different

lengths were designed. Based on the fact that alkylation of the piperidine nitrogen, having no deleterious effects on bioactivity, is an acceptable modification of CD4 mimic analogs, the alkylamine moiety was incorporated into the nitrogen atom of the piperidine moiety to conjugate CD4 mimic analogs with 4F-benzoyl-TZ14011. Reductive alkylation of **4** with *N*<sup>α</sup>-Boc-pyrrolidin-2-ol **24**, which exists in equilibrium with the corresponding aldehyde, and successive treatment with TFA and HCl/dioxane provided the amine hydrochloride **25**. Treatment of **25** with succinic anhydride under basic condition gave the corresponding acid **26**, which was subjected to condensation with the side chain of *D*-Lys<sup>8</sup> of 4F-benzoyl-TZ14011 in an EDC–HOBt system to give the desired hybrid molecule **27** with a tetramethylene linker.<sup>11</sup> Other hybrid molecules **28** and **29** bearing hexa- and octamethylene linkers, respectively, were prepared using the corresponding aldehydes **30** and **31**.

The assay results for these hybrid molecules **27–29** are shown in Table 3. To investigate the effect of conjugation of two molecules on binding activity against CXCR4, the inhibitory potency against





**Scheme 4.** Synthesis of hybrid molecules **27–29**. Reagents and conditions: (a)  $\text{NaBH}(\text{OAc})_3$ ,  $\text{AcOH}$ ,  $\text{DCE}$ ; (b)  $\text{TFA}$ , then  $4\text{ M HCl}/1,4\text{-dioxane}$ ; (c) succinic anhydride, pyridine,  $\text{DMF}$ , then  $4\text{ M HCl}/1,4\text{-dioxane}$ ; (d) 4F-benzoyl-TZ14011,  $\text{EDC}\cdot\text{HCl}$ ,  $\text{HOBt}\cdot\text{H}_2\text{O}$ ,  $\text{Et}_3\text{N}$ ,  $\text{DMF}$ .  $\text{Nal}$  = L-3-(2-naphthyl)alanine,  $\text{Cit}$  = L-citrulline.

**Table 3**  
CXCR4-binding activity, anti-HIV activity and cytotoxicity of hybrid molecules **27–29**<sup>a</sup>

Compd	$\text{EC}_{50}^b$ ( $\mu\text{M}$ )	$\text{IC}_{50}^c$ ( $\mu\text{M}$ )	$\text{CC}_{50}^d$ ( $\mu\text{M}$ )	SI ( $\text{CC}_{50}/\text{IC}_{50}$ )
4F-benzoyl-TZ14011	0.0059	0.0131	ND	ND
<b>1</b> (NBD-556)	ND	0.210	ND	19.2 <sup>e</sup>
<b>27</b> (C4)	0.0044	0.0509	8.60	169
<b>28</b> (C6)	0.0187	0.0365	8.00	219
<b>29</b> (C8)	0.0071	0.0353	8.60	244
AZT	ND	0.0493	ND	ND

<sup>a</sup> All data with standard deviation are the mean values for at least three independent experiments.

<sup>b</sup>  $\text{EC}_{50}$  values are based on the inhibition of [ $^{125}\text{I}$ ]-SDF-1 $\alpha$  binding to CXCR4 transfectants of CHO cells.

<sup>c</sup>  $\text{IC}_{50}$  values are based on the inhibition of HIV-1-induced cytopathogenicity in MT-2 cells.

<sup>d</sup>  $\text{CC}_{50}$  values are based on the reduction of the viability of mock-infected MT-2 cells.

<sup>e</sup> This value is based on the  $\text{CC}_{50}$  and  $\text{IC}_{50}$  values from Table 1.

binding of [ $^{125}\text{I}$ ]-SDF-1 $\alpha$  to CXCR4 was measured. All the hybrid molecules **27–29** significantly inhibited the SDF-1 $\alpha$  binding to CXCR4. The corresponding  $\text{EC}_{50}$  values are:  $\text{EC}_{50}(\mathbf{27}) = 0.0044\ \mu\text{M}$ ;  $\text{EC}_{50}(\mathbf{28}) = 0.0187\ \mu\text{M}$ ;  $\text{EC}_{50}(\mathbf{29}) = 0.0071\ \mu\text{M}$ . These potencies are comparable to that of 4F-benzoyl-TZ14011 ( $\text{EC}_{50} = 0.0059\ \mu\text{M}$ ), indicating that introduction of the CD4 mimic analog into the D-Lys<sup>8</sup> residue of 4F-benzoyl-TZ14011 does not affect binding activity against CXCR4. Comparison of the binding activities of **27–29** showed that all hybrid molecules were essentially equipotent in inhibition of the binding of SDF-1 $\alpha$  to CXCR4. This observation indicates that the linker length between two molecules has no effect on the binding inhibition.

Anti-HIV activity based on the inhibition of HIV-1 entry into the target cells was examined by the MTT assay using a IIIIB(X4) strain. In this assay, the  $\text{IC}_{50}$  value of 4F-benzoyl-TZ14011 was  $0.0131\ \mu\text{M}$ . All hybrid molecules **27–29** showed significant anti-HIV activity [ $\text{IC}_{50}(\mathbf{27}) = 0.0509\ \mu\text{M}$ ;  $\text{IC}_{50}(\mathbf{28}) = 0.0365\ \mu\text{M}$ ;  $\text{IC}_{50}(\mathbf{29}) = 0.0353\ \mu\text{M}$ ]; however, the potency was 2- to 4-fold lower than that of the parent compound 4F-benzoyl-TZ14011, indicating that the conjugation of CD4 mimic with a CXCR4 antagonist did not provide a significant synergistic effect. In view of the fact that the combination uses of CD4 mimic with T140 produced a highly remarkable

synergistic effect, the lower potency of hybrid molecules may be attributed to the inadequacy in the structure and/or the characters of the linkers. All the hybrid molecules **27–29** have relatively strong cytotoxicity [ $\text{CC}_{50}(\mathbf{27}) = 8.6\ \mu\text{M}$ ;  $\text{CC}_{50}(\mathbf{28}) = 8.0\ \mu\text{M}$ ;  $\text{CC}_{50}(\mathbf{29}) = 8.6\ \mu\text{M}$ ]. However, selectivity indexes ( $\text{SI} = \text{CC}_{50}/\text{IC}_{50}$ ) were 169 for **27**, 219 for **28**, and 244 for **29**, all 9–13 times higher than that of **1** ( $\text{SI} = 9.2$ ). This result indicates that conjugation of a CD4 mimic analog with a selective CXCR4 antagonist can improve the SI of CD4 mimic.

The SAR study of a series of CD4 mimic analogs was conducted to investigate the contribution of the piperidine moiety of **1** to anti-HIV activity, cytotoxicity, and CD4 mimicry on conformational changes of gp120. The results indicate that (i) the methyl groups on the piperidine ring of **1** have no great influence on the activities of CD4 mimic; (ii) the presence of piperidine moiety is important for the CD4 mimicry; and (iii) N-substituents of the piperidine moiety contribute significantly to anti-HIV activity and cytotoxicity, as observed with N-alkyl groups such as methyl and isobutyl groups which show moderate anti-HIV activity and lower cytotoxicity.

Several hybrid molecules based on conjugation of a CD4 mimic with a selective CXCR4 antagonist were also synthesized and bio-evaluated. All the hybrid molecules showed significant binding activity against CXCR4 comparable to the parent antagonist and exhibited potent anti-HIV activity. Although no significant synergistic effect was observed, conjugation of a CD4 mimic with a selective CXCR4 antagonist might lead to the development of novel type of CD4 mimic-based HIV-1 entry inhibitors, which possess higher selective indexes than a simple CD4 mimic. These results will be useful for the rational design and synthesis of a new type of HIV-1 entry inhibitors. Further structural modification studies of CD4 mimic are the subject of an ongoing project.

#### Acknowledgements

This work was supported by Grant-in-Aid for Scientific Research from the Ministry of Education, Culture, Sports, Science, and Technology of Japan, Japan Human Science Foundation, and Health and Labour Sciences Research Grants from Japanese Ministry of Health, Labor, and Welfare. T.T. and N.O. are grateful for the JSPS Research Fellowships for Young Scientist.



## References and notes

- Chan, D. C.; Kim, P. S. *Cell* **1998**, *93*, 681.
- (a) Alkhatib, G.; Combadiere, C.; Broder, C. C.; Feng, Y.; Kennedy, P. E.; Murphy, P. M.; Berger, E. A. *Science* **1996**, *272*, 1955; (b) Choe, H.; Farzan, M.; Sun, Y.; Sullivan, N.; Rollins, B.; Ponath, P. D.; Wu, L.; Mackay, C. R.; LaRosa, G.; Newman, W.; Gerard, N.; Gerard, C.; Sodroski, J. *Cell* **1996**, *85*, 1135; (c) Deng, H. K.; Liu, R.; Ellmeier, W.; Choe, S.; Unutmaz, D.; Burkhart, M.; Marzio, P. D.; Marmon, S.; Sutton, R. E.; Hill, C. M.; Davis, C. B.; Peiper, S. C.; Schall, T. J.; Littman, D. R.; Landau, N. R. *Nature* **1996**, *381*, 661; (d) Doranz, B. J.; Rucker, J.; Yi, Y. J.; Smyth, R. J.; Samson, M.; Peiper, S. C.; Parmentier, M.; Collman, R. G.; Doms, R. W. *Cell* **1996**, *85*, 1149; (e) Dragic, T.; Litwin, V.; Allaway, G. P.; Martin, S. R.; Huang, Y.; Nagashima, K. A.; Cayanan, C.; Maddon, P. J.; Koup, R. A.; Moore, J. P.; Paxton, W. A. *Nature* **1996**, *381*, 667.
- Feng, Y.; Broder, C. C.; Kennedy, P. E.; Berger, E. A. *Science* **1996**, *272*, 872.
- (a) Zhao, Q.; Ma, L.; Jiang, S.; Lu, H.; Liu, S.; He, Y.; Strick, N.; Neamati, N.; Debnath, A. K. *Virology* **2005**, *339*, 213; (b) Schön, A.; Madani, N.; Klein, J. C.; Hubicki, A.; Ng, D.; Yang, X.; Smith, A. B., III; Sodroski, J.; Freire, E. *Biochemistry* **2006**, *45*, 10973; (c) Madani, N.; Schön, A.; Princiotta, A. M.; LaLonde, J. M.; Courter, J. R.; Soeta, T.; Ng, D.; Wang, L.; Brower, E. T.; Xiang, S.-H.; Do Kwon, Y.; Huang, C.-C.; Wyatt, R.; Kwong, P. D.; Freire, E.; Smith, A. B., III; Sodroski, J. *Structure* **2008**, *16*, 1689; (d) Haim, H.; Si, Z.; Madani, N.; Wang, L.; Courter, J. R.; Princiotta, A.; Kassa, A.; DeGrace, M.; McGee-Estrada, K.; Mefford, M.; Gabuzda, D.; Smith, A. B., III; Sodroski, J. *ProS Pathogens* **2009**, *5*, 1; (e) Yamada, Y.; Ochiai, C.; Yoshimura, K.; Tanaka, T.; Ohashi, N.; Narumi, T.; Nomura, W.; Harada, S.; Matsushita, S.; Tamamura, H. *Bioorg. Med. Chem. Lett.* **2010**, *20*, 354; (f) Yoshimura, K.; Harada, S.; Shibata, J.; Hatada, M.; Yamada, Y.; Ochiai, C.; Tamamura, H.; Matsushita, S. *J. Virol.* **2010**, *84*, 7558.
- Protein Data Bank (PDB) (entry 1RZJ).
- Olofson, R. A.; Abbott, D. E. *J. Org. Chem.* **1984**, *49*, 2795.
- The synthesis of compound **4**: To the solution of compound **10** (104 mg, 0.52 mmol) in dry THF (4.0 mL), Et<sub>3</sub>N (159  $\mu$ L, 1.15 mmol), HOBt·H<sub>2</sub>O (87 mg, 0.57 mmol), EDCI-HCl (109 mg, 0.57 mmol) and 4-amino-1-benzylpiperidine (109  $\mu$ L, 0.57 mmol) were added with stirring at 0 °C, and continuously stirred for 6 h with warming to room temperature under N<sub>2</sub> atmosphere. After concentration under reduced pressure, the residue was extracted with EtOAc. The extract was washed with aq saturated NaHCO<sub>3</sub> and brine, and dried over MgSO<sub>4</sub>. Concentration under reduced pressure followed by flash chromatography over silica gel with CHCl<sub>3</sub>-MeOH (20:1) including 1% Et<sub>3</sub>N gave the crude benzyl amine as a white powder. To the solution of the above crude benzyl amine (95 mg, 0.26 mmol) in dry CH<sub>2</sub>Cl<sub>2</sub> (10 mL), 1-chloroethyl chloroformate (110  $\mu$ L, 0.68 mmol) was added dropwise with stirring at 0 °C. The mixture was then refluxed for 3 h under N<sub>2</sub> atmosphere. After concentration under reduced pressure, the residue was resolved in MeOH (10 mL) and then refluxed for 1 h. Concentration under reduced pressure gave a crude product. Reprecipitation with MeOH-Et<sub>2</sub>O afforded a white powder of the title compound **4** (33 mg, 46% yield).  $\delta_{\text{H}}$  (400 MHz; CD<sub>3</sub>OD) 1.83–1.92 (2H, m, CH<sub>2</sub>), 2.10–2.17 (2H, m, CH<sub>2</sub>), 3.13 (2H, t, J 12.5, CH<sub>2</sub>), 3.34 (1H, m, NH), 3.42–3.49 (1H, m, CH<sub>2</sub>), 4.04 (1H, m, CH), 7.34 (2H, m, ArH), 7.51 (1H, m, NH), 7.73 (2H, m, ArH), 8.84 (1H, m, NH); LRMS (ESI), *m/z* calcd for C<sub>13</sub>H<sub>17</sub>ClN<sub>2</sub>O<sub>2</sub> (MH)<sup>+</sup> 282.10, found 282.14.
- Yoshimura, K.; Shibata, J.; Kimura, T.; Honda, A.; Maeda, Y.; Koito, A.; Murakami, T.; Mitsuya, H.; Matsushita, S. *AIDS* **2006**, *20*, 2065.
- (a) Tamamura, H.; Xu, Y.; Hattori, T.; Zhang, X.; Arakaki, R.; Kanbara, K.; Omagari, A.; Otaka, A.; Ibuka, T.; Yamamoto, N.; Nakashima, H.; Fujii, N. *Biochem. Biophys. Res. Commun.* **1998**, *253*, 877; (b) Tamamura, H.; Hiramatsu, K.; Mizumoto, M.; Ueda, S.; Kusano, S.; Terakubo, S.; Akamatsu, M.; Yamamoto, N.; Trent, J. O.; Wang, Z.; Peiper, S. C.; Nakashima, H.; Otaka, A.; Fujii, N. *Org. Biomol. Chem.* **2003**, *1*, 3663.
- Hanaoka, H.; Mukai, T.; Tamamura, H.; Mori, T.; Ishino, S.; Ogawa, K.; Iida, Y.; Doi, R.; Fujii, N.; Saji, H. *Nucl. Med. Biol.* **2006**, *33*, 489.
- The synthesis of a hybrid molecule **27**: To the solution of compound **26** (2.6 mg, 4.6  $\mu$ mol) in DMF (1.0 mL), Et<sub>3</sub>N (26  $\mu$ L, 92  $\mu$ mol), HOBt·H<sub>2</sub>O (3.5 mg, 23  $\mu$ mol) and EDCI-HCl (4.5 mg, 23  $\mu$ mol) were added with stirring at 0 °C, and stirred for 1 h at room temperature. To the mixture 4F-benzoyl-TZ14011 (15 mg, 4.1  $\mu$ mol) was then added and the mixture was stirred for 24 h at room temperature under N<sub>2</sub> atmosphere. After concentration under reduced pressure, the residue was purified by reversed phase HPLC (*t<sub>R</sub>* = 23 min, elution: a linear gradient of 27–31% acetonitrile containing 0.1% TFA over 30 min) to afford a fluffy white powder of the desired compound **27** (1.3 mg, 9.8%). LRMS (ESI), *m/z* 2621.20 [M+H]<sup>+</sup>, calcd 2620.25.

# Remodeling of Dynamic Structures of HIV-1 Envelope Proteins Leads to Synthetic Antigen Molecules Inducing Neutralizing Antibodies

Toru Nakahara,<sup>†</sup> Wataru Nomura,<sup>\*,†</sup> Kenji Ohba,<sup>‡</sup> Aki Ohya,<sup>†</sup> Tomohiro Tanaka,<sup>†</sup> Chie Hashimoto,<sup>†</sup> Tetsuo Narumi,<sup>†</sup> Tsutomu Murakami,<sup>‡</sup> Naoki Yamamoto,<sup>‡</sup> and Hirokazu Tamamura<sup>\*,†</sup>

Department of Medicinal Chemistry, Institute of Biomaterials and Bioengineering, Tokyo Medical and Dental University, 2-3-10 Kandasurugadai, Chiyoda-ku, Tokyo 101-0062, Japan, and AIDS Research Center, National Institute of Infectious Diseases, 1-23-1 Toyama, Shinjuku-ku, Tokyo 162-8640, Japan. Received November 16, 2009; Revised Manuscript Received February 28, 2010

A synthetic antigen targeting membrane-fusion mechanism of HIV-1 has a newly designed template with C3-symmetric linkers mimicking N36 trimeric form. The antiserum produced by immunization of the N36 trimeric form antigen showed structural preference in binding to N36 trimer and stronger inhibitory activity against HIV-1 infection than the N36 monomer. Our results suggest an effective strategy of HIV vaccine design based on a relationship to the native structure of proteins involved in HIV fusion mechanisms.

## INTRODUCTION

Antibody-based therapy is one of the promising treatments for AIDS. In recent years, AIDS antibodies have been produced by immunization (1) and by de novo engineering of monoclonal antibodies (mAb) with molecular evolution tactics such as phage display (2). Despite enormous efforts, however, only a limited number of highly and broadly HIV-neutralizing human mAbs have been isolated and characterized. These antibodies include gp41 Abs, 2F5 (3–6) and 4E10 (5–7), and gp120 Abs, 2G12 (8) and b12 (9). gp41 is a transmembrane envelope glycoprotein, which is divided into an endodomain and an ectodomain by the transmembrane region; the latter contains a hydrophobic amino-terminal fusion peptide, followed by amino-terminal and carboxy-terminal leucine/isoleucine heptad repeat domains with helical structures (HR1 and HR2, respectively). In the membrane fusion process of HIV-1, these subunits form a “pre-bundle” complex. The HR1 and HR2 regions are termed the N-terminal helix (N36) and C-terminal helix (C34), respectively. These helices form a six-helical bundle consisting of a central parallel trimeric coiled-coil of N36 surrounded by C34 in an antiparallel hairpin fashion. In design of immunogens that elicit broadly neutralizing antibodies, a useful strategy is to produce molecules that mimic the natural trimer on the virion surface. Previous studies show that these molecules could be proteins expressed as a recombinant form or on the surface of particles such as pseudovirions or proteoliposomes (10–12). The X-ray crystallographic study of gp41 shows that the distances between any two residues at the N-terminus of N-region are almost equal at approximately 10 Å (Figure 1A). A chemically synthetic template could be useful in connection with the design of a peptidomimetic corresponding to the native structure of gp41. To date, several gp41 mimetics have been synthesized as inhibitors or antigens and subjected to inhibition or neutralization assays (13–16). However, the templates for assembly of these helical peptides contain branched peptide linkers, which are not exactly equivalent in length (14). The N-terminal peptides constrained by another threefold linker showed high affinity for

C-terminal peptides, although its biological advantages have not been determined (15). The mimicry can be estimated using the broadly neutralizing mAbs; suitable mimetics will bind neutralizing mAbs efficiently, but they will bind non-neutralizing mAbs poorly. In the present study, we designed and synthesized a novel three-helical bundle mimetic, which corresponds to the trimeric form of N36. We investigated whether mice immunized with the equivalent trimeric form of N36 mimetic can produce antibodies with stronger binding affinity for N36 trimer than for N36 monomer. This approach demonstrates the possibility of producing structure-specific antibodies by immunization of synthetic antigens corresponding to the natural form of viral proteins.

## EXPERIMENTAL PROCEDURES

**Conjugation of N36REGC and the Template to Produce triN36e.** Compound 6 (100 µg, 0.174 µmol) and N36REGC (3.4 mg, 0.574 µmol) were dissolved in a mixture of 300 µL of 200 mM acetate buffer (pH 5.2) and 300 µL of TFE under a nitrogen atmosphere, then TCEP·HCl was added. The reaction was stirred for 72 h at room temperature and monitored by HPLC. The ligation product (triN36e) was separated as an HPLC peak and was characterized by ESI-TOF-MS, *m/z* calcd for C<sub>690</sub>H<sub>1160</sub>N<sub>226</sub>O<sub>201</sub>S<sub>3</sub> 15933.1, found 15933.8. The purification was performed by reverse phase HPLC (YMC-Pack ODS-A column, 10 × 250 mm). Elution was carried out with a 40–50% linear gradient of acetonitrile (0.1% TFA) over 50 min. Purified triN36e, obtained in 16% yield, was identified by ESI-TOF-MS. The detailed synthesis of peptides is described in the Supporting Information (SI).

**CD Spectra.** CD measurements were performed with a J-720 circular dichroism spectropolarimeter equipped with a thermoregulator (JASCO). The wavelength dependence of molar ellipticity [θ] was monitored at 25 °C from 190 to 250 nm. Peptides were dissolved in 20 mM acetate buffer (pH 4.0) containing 40% MeOH (23, 24). The experimental helicity was calculated as reported previously (17–19).

**Immunization and Sample Collection.** Six-week-old male BALB/c mice were purchased from Sankyo Laboratory Service Corp. (Tokyo, Japan) and maintained under specific pathogen-free conditions in an animal facility. The experimental protocol was approved by the ethical review committee of Tokyo Medical and Dental University. Freund incomplete adjuvant and PBS

\* To whom correspondence should be addressed. E-mail: nomura.mr@tmd.ac.jp; tamamura.mr@tmd.ac.jp. phone: +81-3-5280-8036, fax: +81-3-5280-8039.

<sup>†</sup> Tokyo Medical and Dental University.

<sup>‡</sup> National Institute of Infectious Diseases.